The Abdus Salam
International Centre for Theoretical Physics

United Nations
Educational, Scientific
and Cultural Organization

International Atomic
Energy Agency

310/1749-50

ICTP-COST-USNSWP-CAWSES-INAF-INFN
International Advanced School
on
Space Weather
2-19 May 2006

The Cosmic Ray Record

Claudio TUNIZ
The Abdus Salam International Centre for
Theoretical Physics (ICTP)
Trieste
ITALY

These lecture notes are intended only for distribution to participants

The cosmic ray record

Claudio Tuniz

The Abdus Salam International Centre for Theoretical Physics,
Trieste, Italy

A nuclear physicist's viewpoint

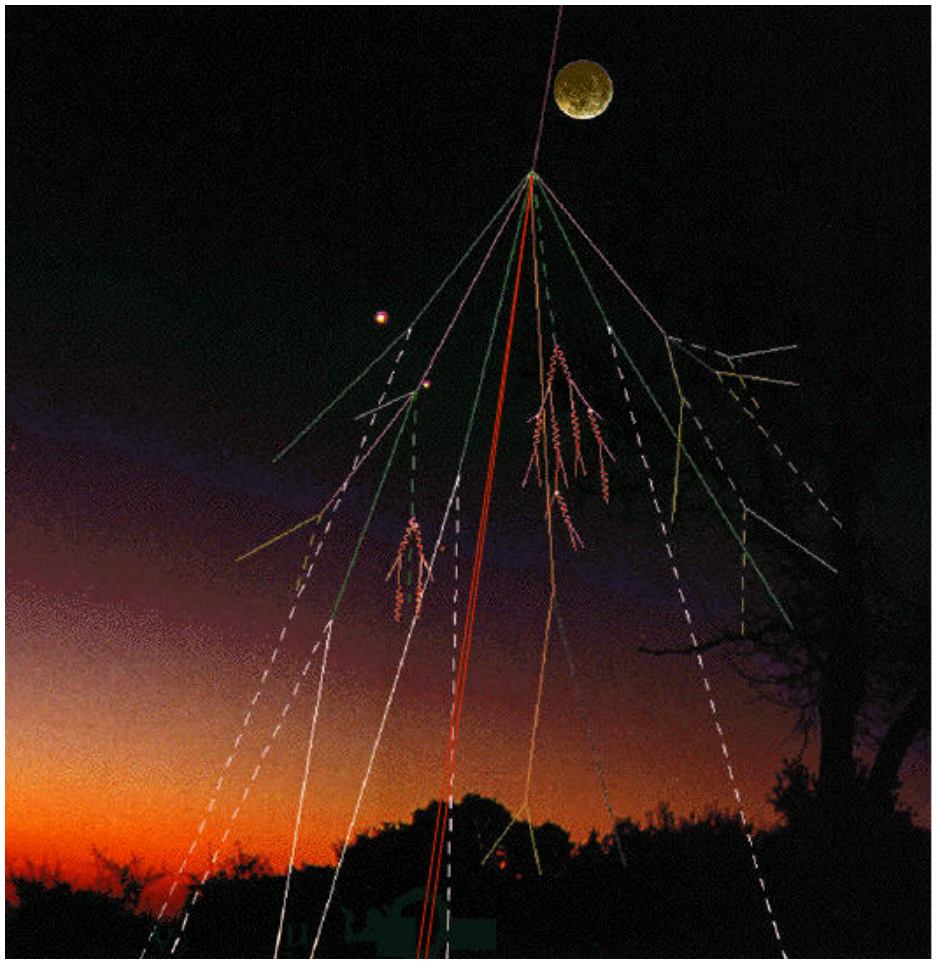

Lecture outline:

- Cosmic rays (ion beam)
- Solar system matter (target)
- Nuclear reactions (radionuclide production)
- Counting rare radio-nuclides
- Extraterrestrial archives
- Terrestrial archives
- Solar variability

Cosmic rays: history

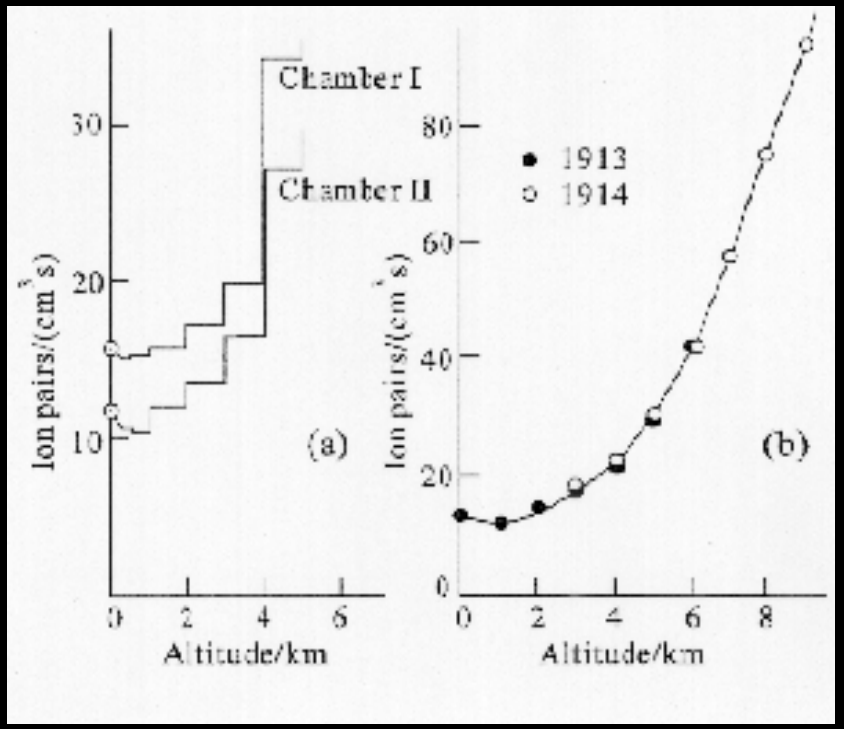

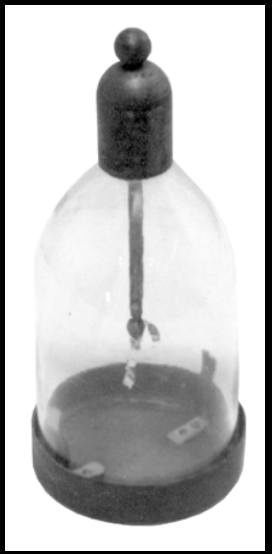

Cosmic ray: history

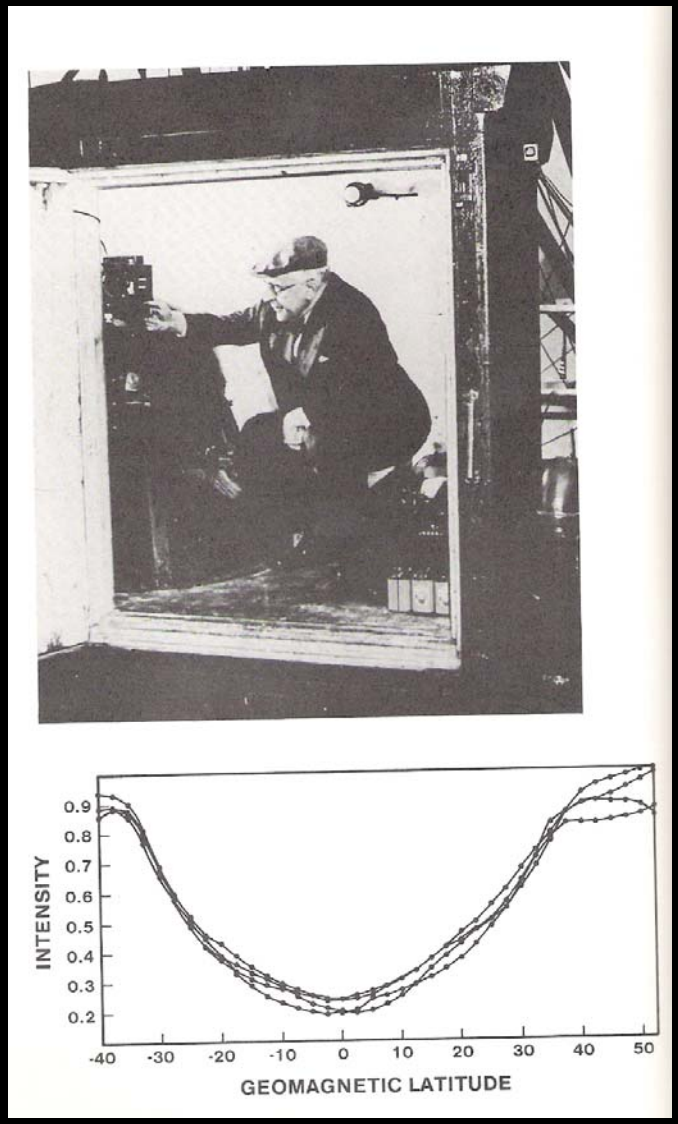

From M W Friedlande, Cosmic Rays

Last generation CR detectors

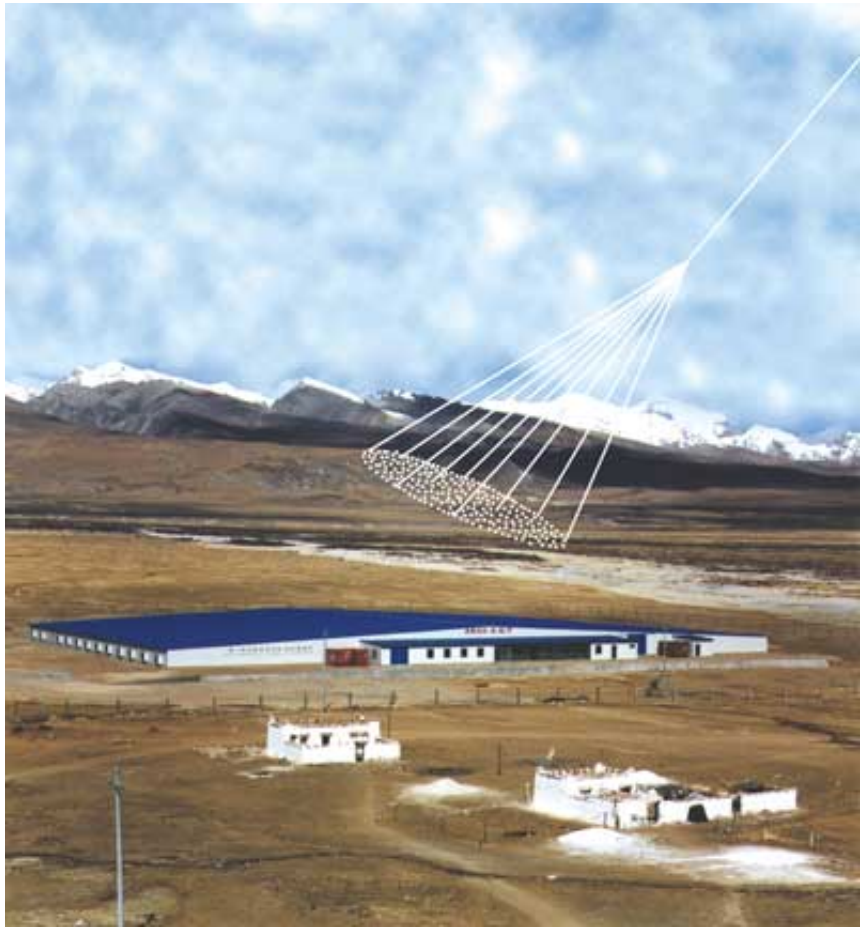

ARGO experiment in Tibet. A simulated particle shower strikes the ARGO detector

18,500 detectors will cover a an area as large as a soccer field.

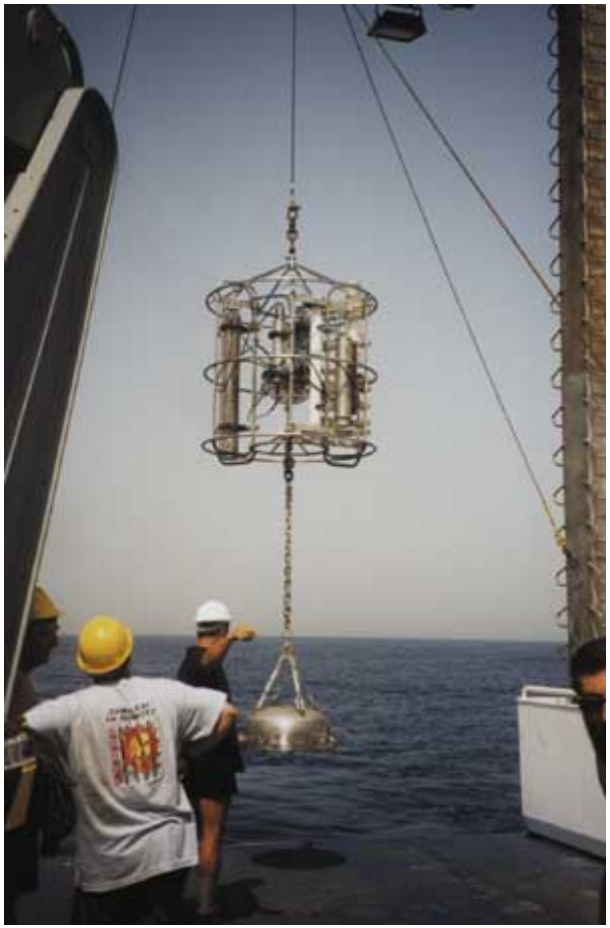

NEMO experiment in Italy. Apparatus to detect the Cerenkov light produced by the passage of neutrinos through water to be installed undersea at a depth of two 5 kilometers .

Cosmic rays: energy and flux

Table 5.1 Comparison of Solar Wind, SCR, and GCR Fluxes

	Solar Wind	SCR	GCR
Nucleon energies	0.3 – 3 keV	~1 – 100 MeV	~0.1 – >10 GeV
Electron energies	~1 – 100 eV	<0.1 – 1 MeV	~0.1 – >10 GeV
Proton fluxes (cm^{-2} sec^{-1})	$\sim 3 \times 10^8$	100	2 – 4
Penetration depth in solid matter	μm	cm	m

Source: Vaniman, D. et al., in *Lunar Sourcebook: A User's Guide to the Moon*, Heiken, D.H. et al., Eds., Cambridge University Press, London, 1991, 27. With permission.

Cosmic rays: elemental abundance

Accelerator mass Spectrometry
C. Tuniz et al., CRC Press, 1998

Table 5.2 Elemental Composition of GCR Compared with the Abundance of the Same Elements in the Universe

Element	Atomic Number	Abundance (%)	
		GCR	Universe
H	1	93	91
He	2	6.3	9.1
Li, Be, B	3 – 5	0.10	0.4
C, N, O, F	6 – 9	0.42	0.14
Ne-K	10 – 19	0.14	0.014
Ca-Zn	20 – 30	0.04	2×10^{-3}
Ga-U	31 – 92	2×10^{-6}	10^{-6}

Source: Pomerantz, M.A. and Duggal, S.P., *Rev. Geophys. Space Phys.*, 12, 243, 1974. With permission.

Cosmic rays: energy spectrum

Accelerator mass Spectrometry
C. Tuniz et al., CRC Press, 1998

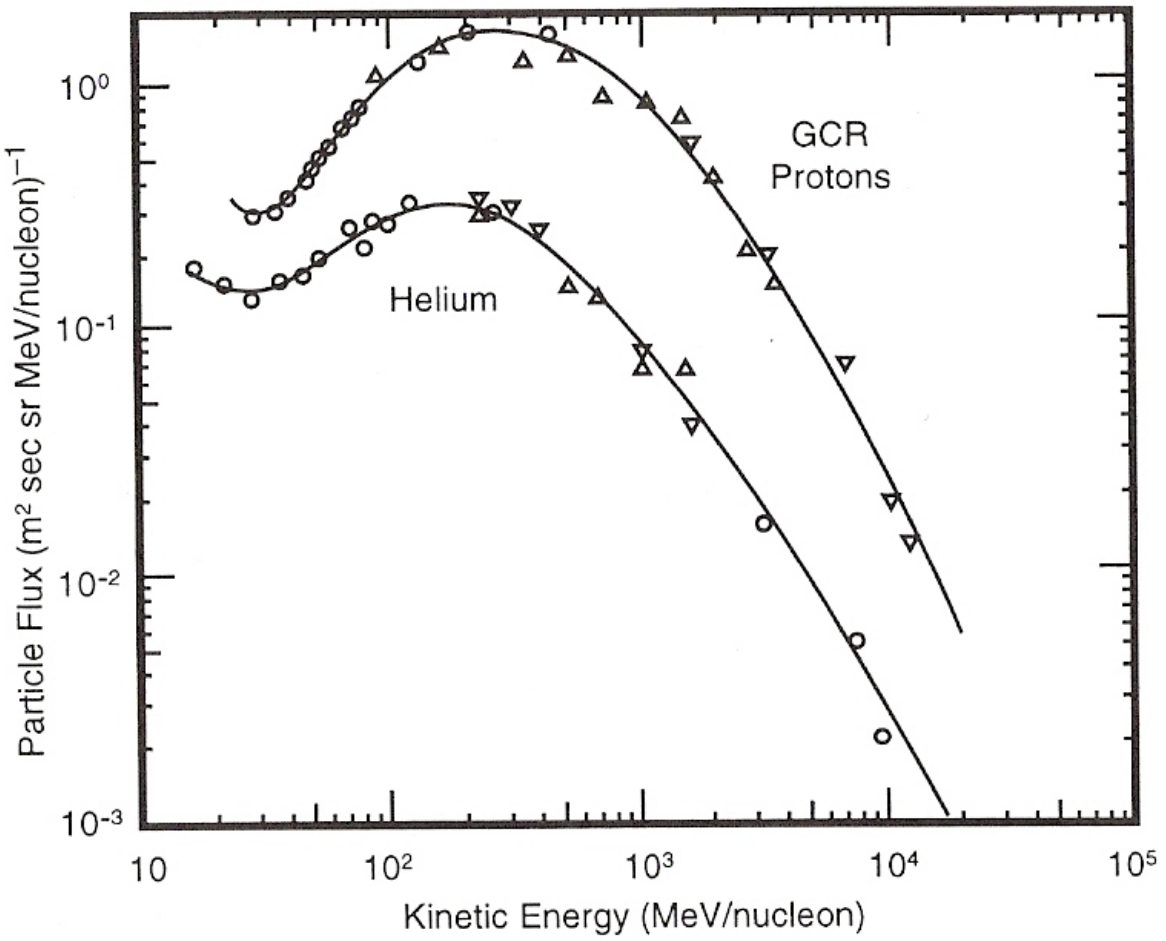

Figure 5.2 The measured energy spectra of GCR proton and helium fluxes at 1 AU.

Galactic modulation

5.4.1 *Galactic modulation*

Galactic cosmic ray variability can result from several processes that are active outside the solar system on time scales on the order of 10^6 to 10^9 years:

- Fluctuations in the activity of the GCR sources
- Changes in acceleration and transport conditions in the interstellar medium during the period of 10^6 to 10^7 years that GCRs may spend in the galactic magnetic field
- Passage of the solar system through interstellar clouds
- Oscillation of the solar system through the galactic plane (Vanzani et al., 1987)

Solar modulation

Accelerator mass Spectrometry
C. Tuniz et al., CRC Press, 1998

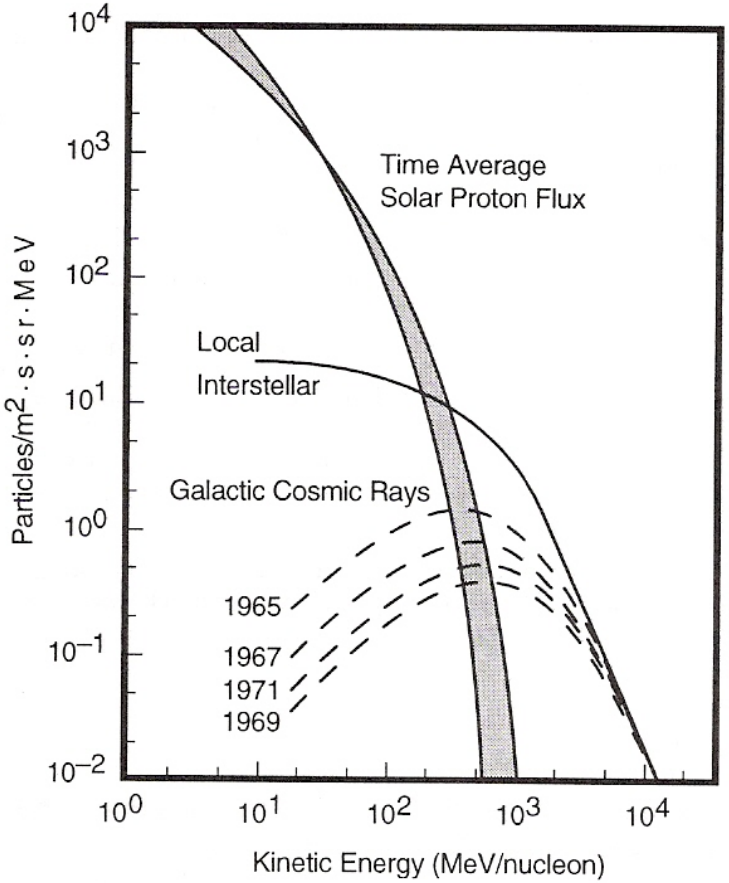

Figure 5.4 Calculated GCR spectra as a function of particle energy showing the effects of solar modulation. For comparison, the calculated GCR spectrum in interstellar space and the time averaged SCR proton flux are also shown. (Adapted from Castagnoli, G. and Lal, D., *Radiocarbon*, 22, 133, 1980; Reedy, R.C. et al., *Ann. Rev. Nucl. Part. Sci.*, 33, 505, 1983.)

Cosmic ray interactions

- Nuclear reactions [light GCR & SCR]
  - Radioactive nuclides [^{10}Be, ^{26}Al, ^{53}Mn,…]
  - Stable nuclides [noble gases]
- Ionization energy loss [SCR, heavy GCR]
  - Nuclear tracks
  - Thermo luminescence
- Implantation [solar wind]

Nuclear reactions by cosmic rays
(radionuclide production)

7.1 Atmospheric production of cosmogenic nuclides

The radionuclide production rate, P(h,θ,t), at altitude, h, and geomagnetic latitude, θ, at time t is given by the general formula:

Production rate

$$P(h,N,t) = \int_E \{\Sigma_k \Sigma_j \theta_k (h,\theta,t,E)\, \sigma_{jk}(E) N_j\}\, dE \qquad (7.1)$$

where:

θ_k = differential energy spectrum of component k of the cosmic ray flux
N_j = atom abundance of target nuclide j in the irradiated material
σ_{jk} = cross-section for the production of the radionuclide in the collision of particle k of energy E with target nuclide j

Accelerator mass Spectrometry
C. Tuniz et al., CRC Press, 1998

Terrestrial production

Accelerator mass Spectrometry
C. Tuniz et al., CRC Press, 1998

Table 7.1 Cosmogenic Radionuclides Produced in Terrestrial Matter

Radionuclide	Half-Life ($t_{1/2}$)	Main Terrestrial Target Elements	
		Atmosphere	Lithosphere
^{3}H	12.3 a	N, O	O, Mg, Si, Fe
^{7}Be	53.3 d	N, O	O, Mg, si, Fe
^{10}Be	1.51 Ma	N, O	O, Si, Mg, Fe
^{14}C	5730 a	N, O	O, Mg, Si, Fe
^{22}Na	2.61 a	Ar	Mg, Al, Si, Fe
^{26}Al	720 ka	Ar	Cl, K, Ca, Fe
^{32}Si	~140 a	Ar	Cl, K, Ca, Fe
^{36}Cl	301 ka	Ar	Cl, K, Ca, Fe
^{39}Ar	269 a	Ar	K, Ca, Fe
^{41}Ca	103 ka	Kr	Ca, Ti, Fe
^{81}Kr	210 ka	Kr	Rb, Sr, Zr
^{90}Sr	28.8 a	Fission	
^{129}I	15.7 Ma	Xe	Te, Ba, Ce, La

Note: The listed isotopes have been measured by AMS or have been proposed to be measured by AMS.

Cosmogenic radionuclides

The rate of production of cosmogenic radionuclides depends on:

1) **latitude**
2) **geomagnetic field strength**
3) **solar activity**

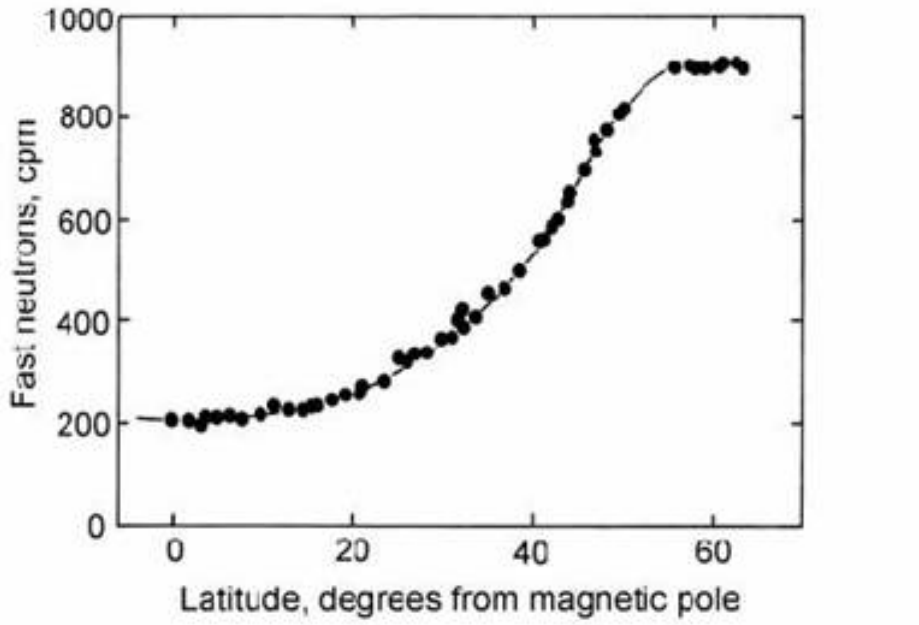

Secondary cosmic rays

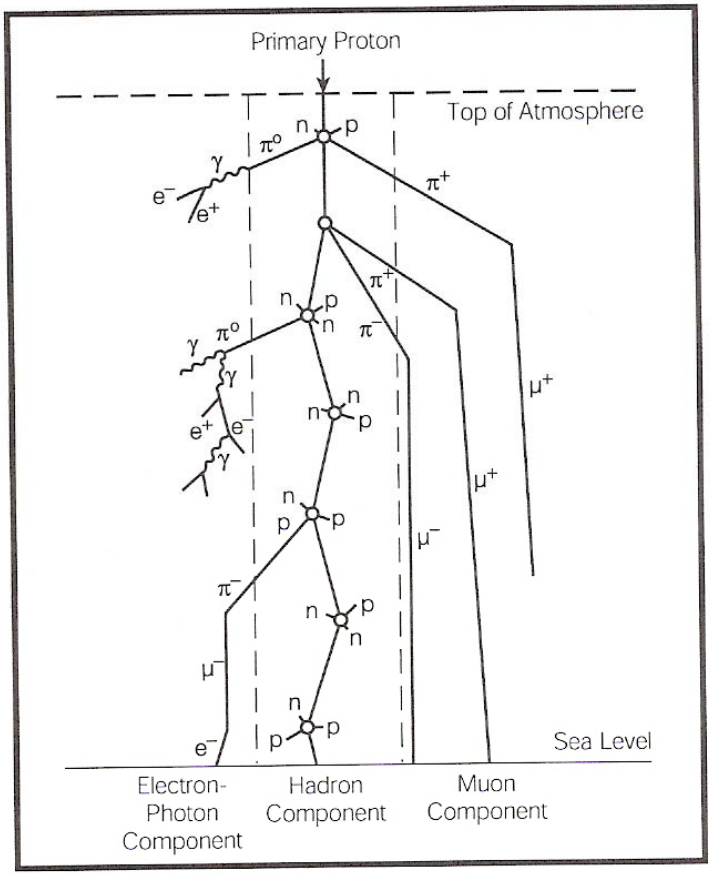

Figure 5.1 Schematic illustration of the development of the secondary cosmic ray flux produced in the atmosphere and the resultant flux at the Earth's surface as a result of galactic cosmic ray bombardment. The three panels show the different particles generated in the electron, hadron (protons and neutrons), and muon components.

Accelerator mass Spectrometry
C. Tuniz et al., CRC Press, 1998

Secondary CR reactions in the lithosphere

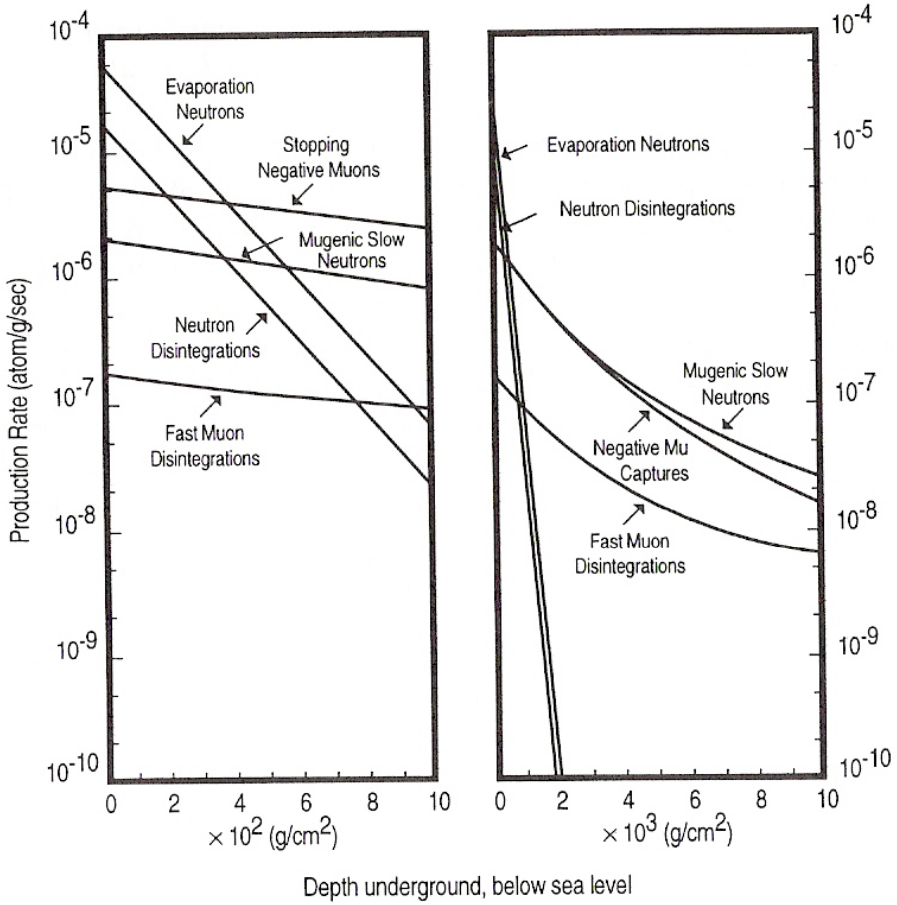

Accelerator mass Spectrometry
C. Tuniz et al., CRC Press, 1998

Figure 7.2 Nuclear interaction rates due to nucleons and muons in the upper layers of the Earth's crust as a function of depth below the surface. The left-hand figure shows the production rate variations on an expanded scale for depths up to about 3 m. (From Lal, D., *Earth Planet. Sci. Lett.*, 104, 424, 1991. With permission.)

Production of cosmogenic isotopes in the lithosphere

Accelerator mass Spectrometry
C. Tuniz et al., CRC Press, 1998

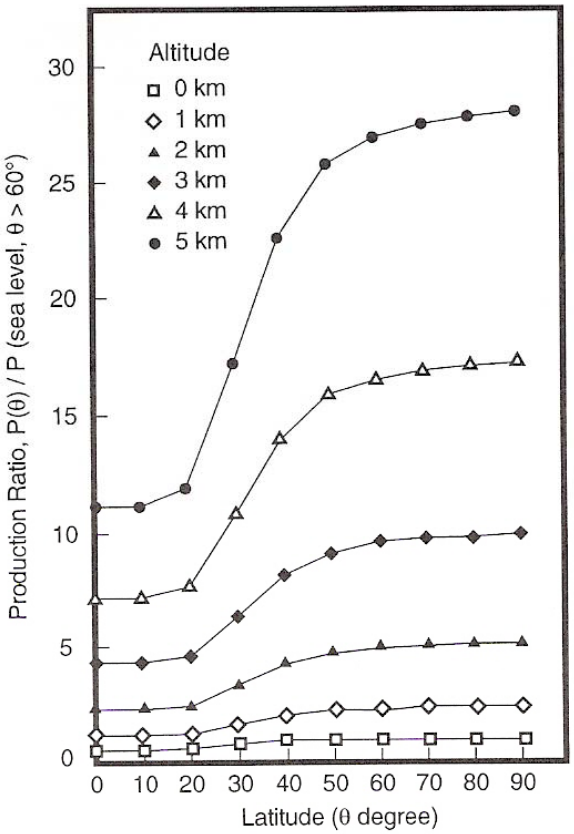

Figure 11.1 Variation of *in situ* production rates as a function of latitude and altitude, P(θ), normalized to the sea-level, high-latitude production rate (P) (latitude > 60°). The polynomial parameterization given by Lal (1991) for latitude and altitude variations of the cosmic ray flux were used (see Figure 7.1). (Courtesy of J. Klein, University of Pennsylvania.)

Production of cosmogenic isotopes in the lithosphere

Accelerator mass Spectrometry
C. Tuniz et al., CRC Press, 1998

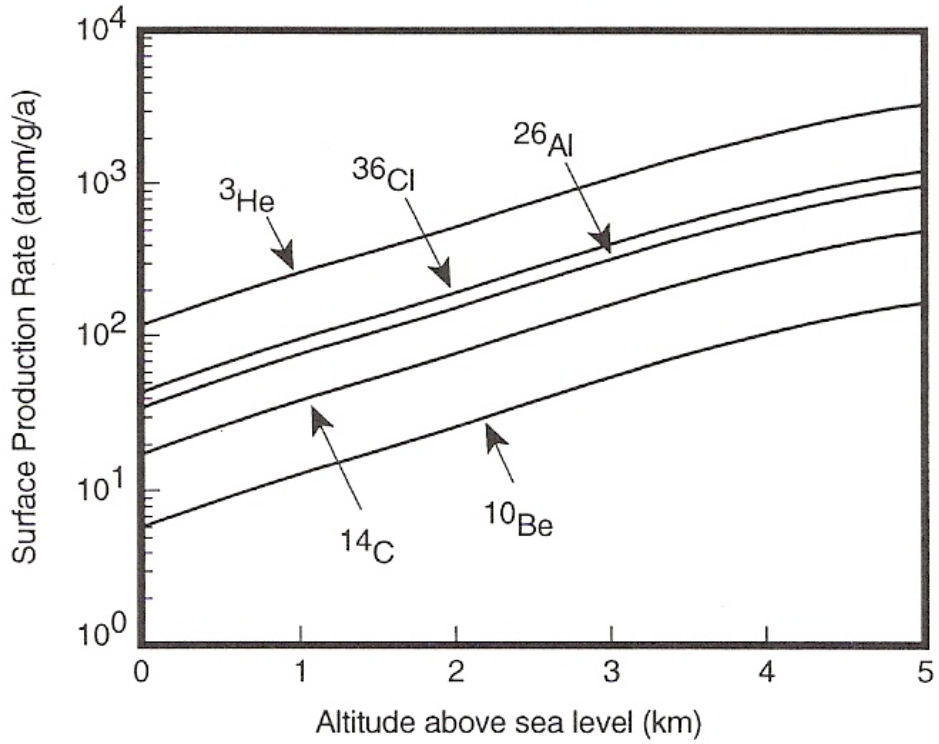

Figure 7.7 Calculated terrestrial production rates of *in situ* cosmogenic nuclides in surface rocks as a function of altitude based on numerical simulation computer codes using an incident GCR proton flux of 4.6 protons/cm^2/sec for energies >10 MeV. The target for ^{36}Cl is CaO and SiO_2 for the others. (From Masarik, J. and Reedy, R.C., *Earth Planet. Sci. Lett.*, 136, 381, 1994. With permission.)

Measured and predicted depth dependence for ^{10}Be and ^{36}Cl (Elmore et al, Purdue University)

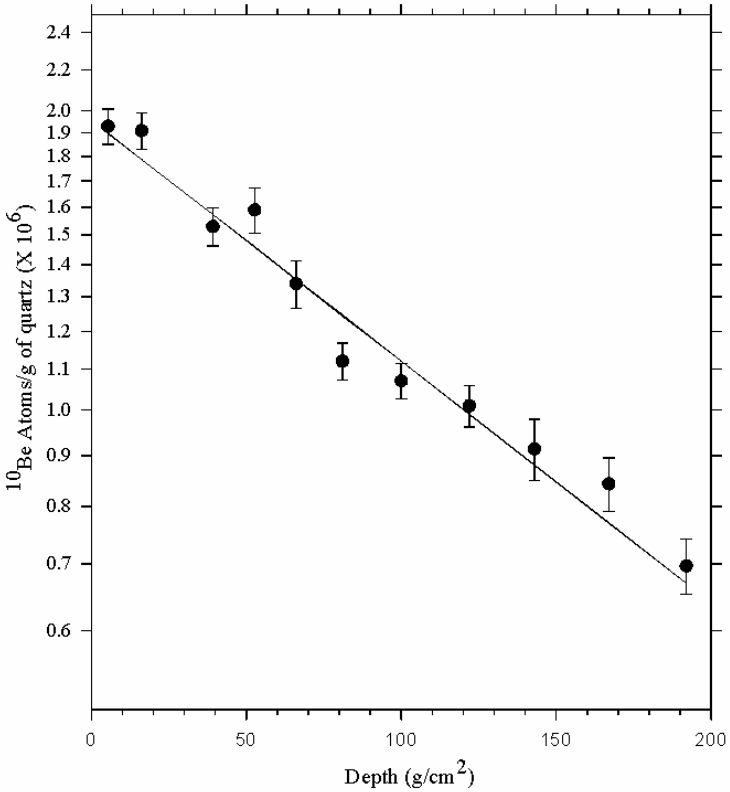

Figure 2

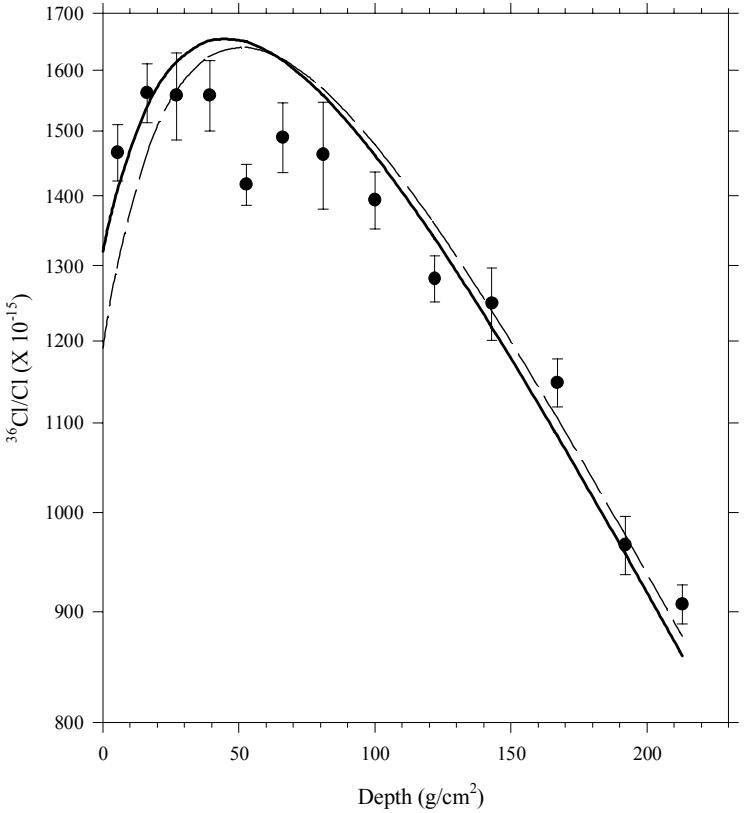

Figure 1

^{36}Cl production in a boulder

Accelerator mass Spectrometry
C. Tuniz et al., CRC Press, 1998

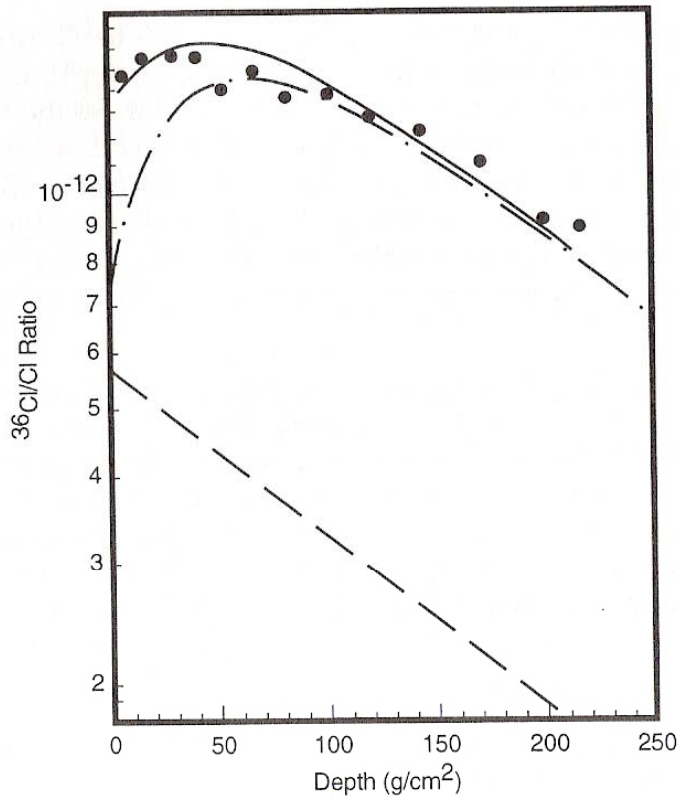

Figure 7.6 Measured and predicted depth dependence of ^{36}Cl/Cl in a 90-cm core taken from a granodiorite erratic boulder at Bishop Creek, California. The solid line is a model calculation normalized to the data points. The dot-dash line is the predicted ratio from production of ^{36}Cl from neutron capture on Cl, and the dashed line is the calculated depth dependence for ^{36}Cl production from spallation on Ca and K. The neutron capture component shows the distinct sub-surface maximum for production from neutrons, and the spallation component results from the exponential reduction in the flux of energetic secondary particles. (From Dep, L., Cosmogenic Radionuclide Production in Terrestrial Rocks: AMS Measurements and Monte Carlo Simulations, Ph.D. thesis, Department of Physics, Purdue University, W. Lafayette, IN, 1995.)

Samples

- Meteorites (asteroids, moon, mars)
- Cosmic dust (stratosphere)
- Cosmic spherules (ocean)
- Lunar samples
- Comet return mission
- Asteroid return mission
- Spacecraft components
  - Surveyor III (Apollo 12)

Cosmic ray nuclear reactions: extraterrestrial material

Production rate

$$P_X(R,d) = \int_E \{\Sigma_k \Sigma_j \phi_k(E,R,d)\sigma_{j,k}(E)N_j\}\, dE \qquad (6.3)$$

Accelerator mass Spectrometry
C. Tuniz et al., CRC Press, 1998

Cosmogenic isotopes on the Moon

Accelerator mass Spectrometry
C. Tuniz et al., CRC Press, 1998

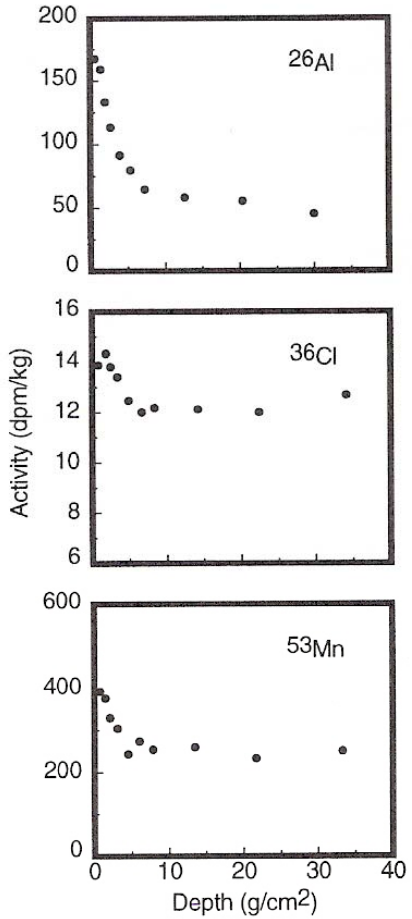

Figure 6.7 Surface profiles of ^{26}Al, ^{36}Cl, and ^{53}Mn in selected lunar cores and rocks. Depth range is from surface to about 15 cm. Activities increase sharply towards the surface, reflecting production by low-energy solar cosmic rays. (Profile of ^{26}Al from Fruchter, J.C. et al., *Proc. 13th Lunar Planet. Sci. Conf.*, 13, 243, 1982; ^{36}Cl from Nishiizumi, K. et al., *Proc. 19th Lunar Planet. Sci. Conf.*, XIX, 305, 1988; ^{53}Mn from Nishiizumi, K. et al., *J. Geophys. Res.*, 88, 211, 1983. With permission.)

Cosmogenic isotopes on the Moon

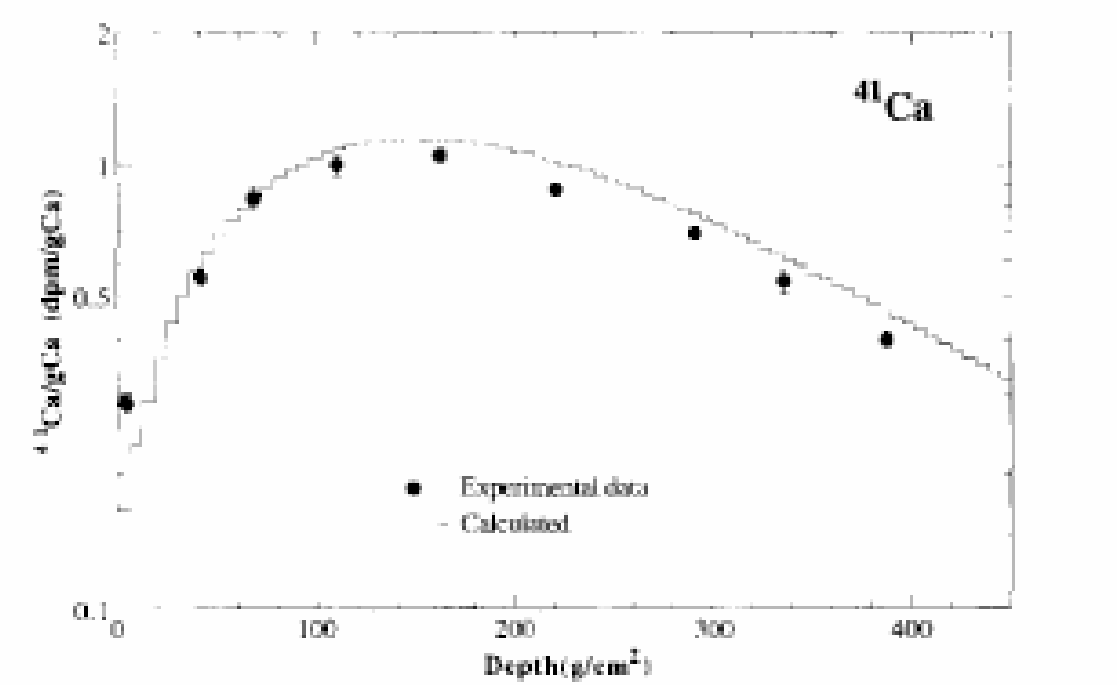

Fig. 2. Low-energy neutron produced ^{41}Ca activities in the Apollo 15 drill core. The experimental data have been normalized to Ca concentrations after subtraction of small amounts of spallation contribution (see text). The solid line is the calculated production rate using the LAHET Code System, assuming ^{41}Ca from ^{40}Ca (n, γ) reaction.

Nishiizumi et al, 1997.

Long-lived cosmogenic radionuclides in solar system matter

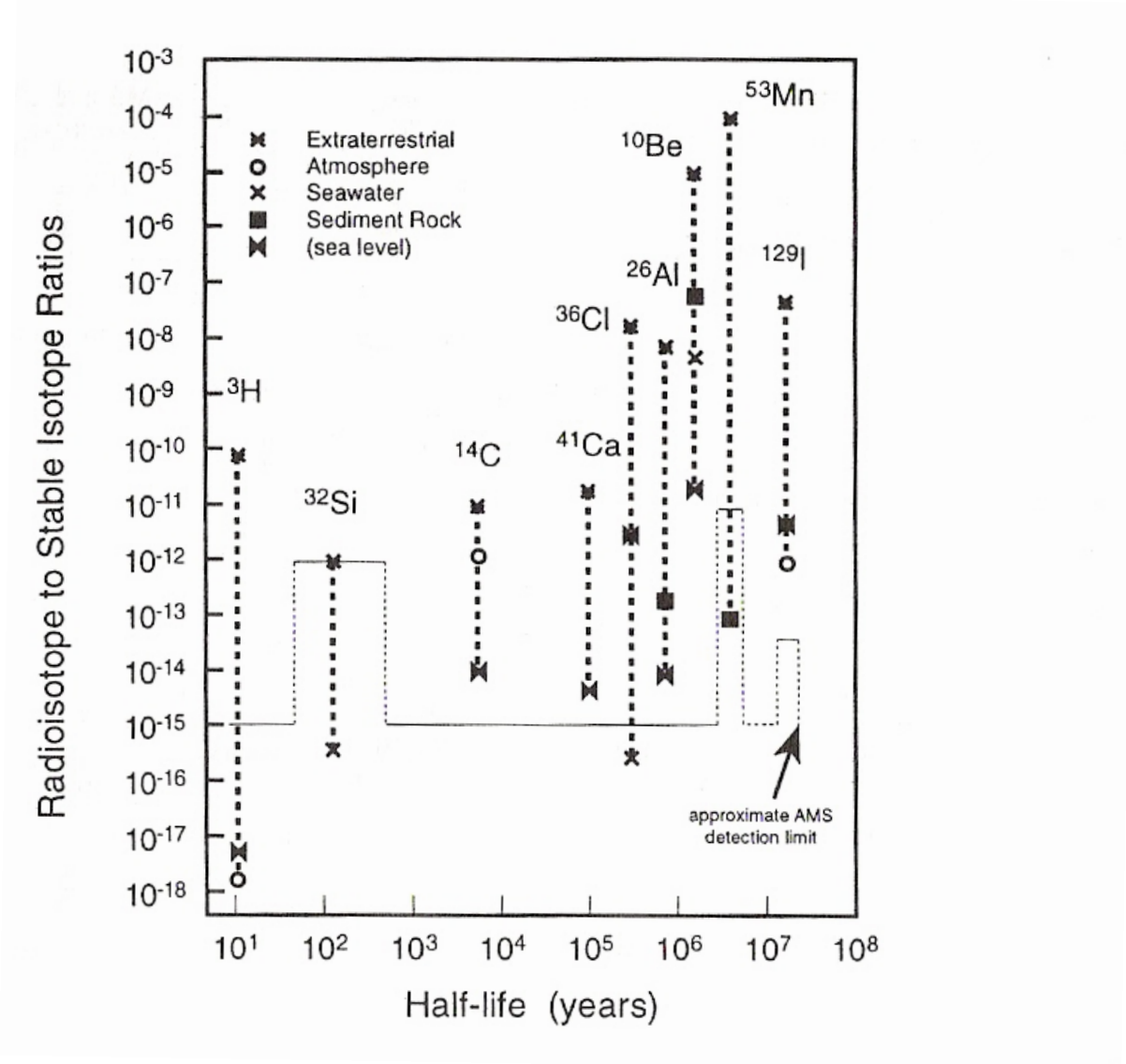

Accelerator mass Spectrometry
C. Tuniz et al., CRC Press, 1998

Counting rare radionuclides before the invention of AMS

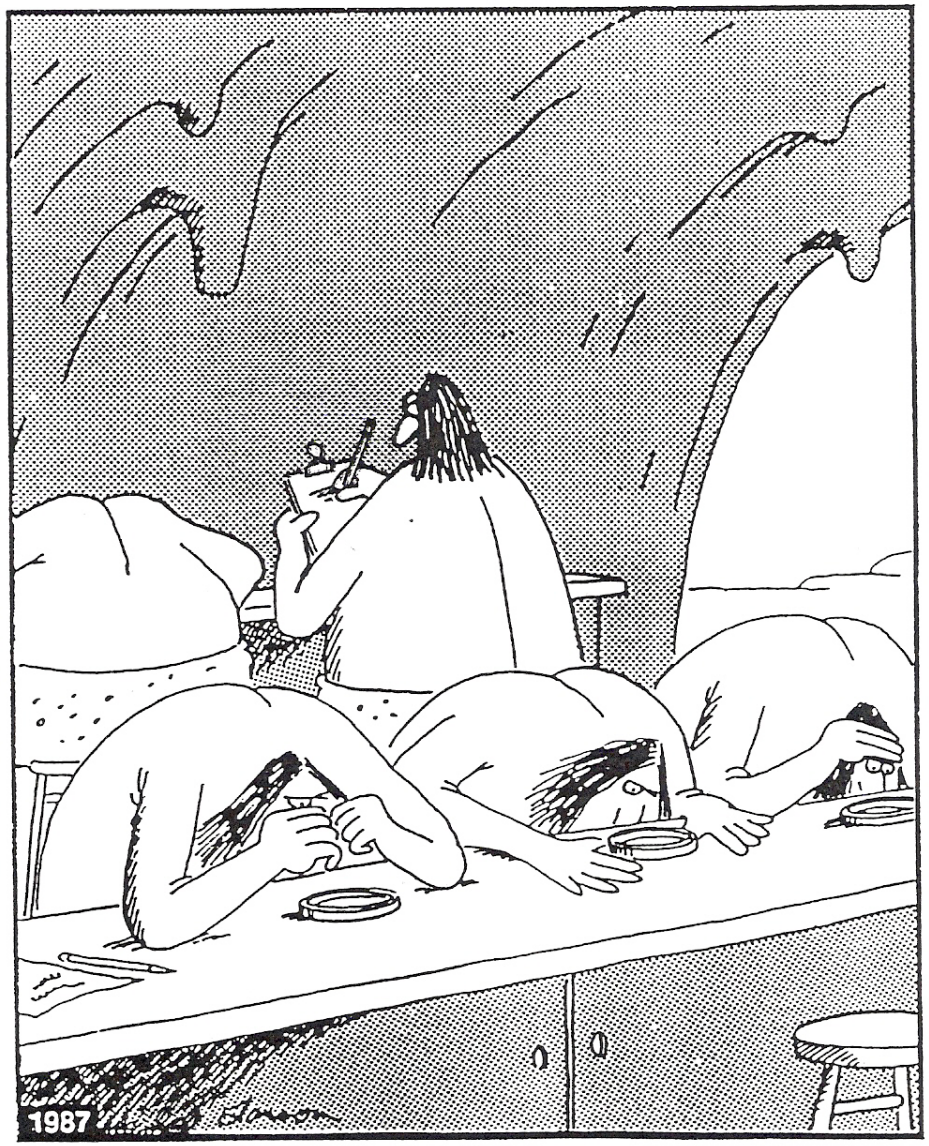

Accelerator Mass Spectrometry

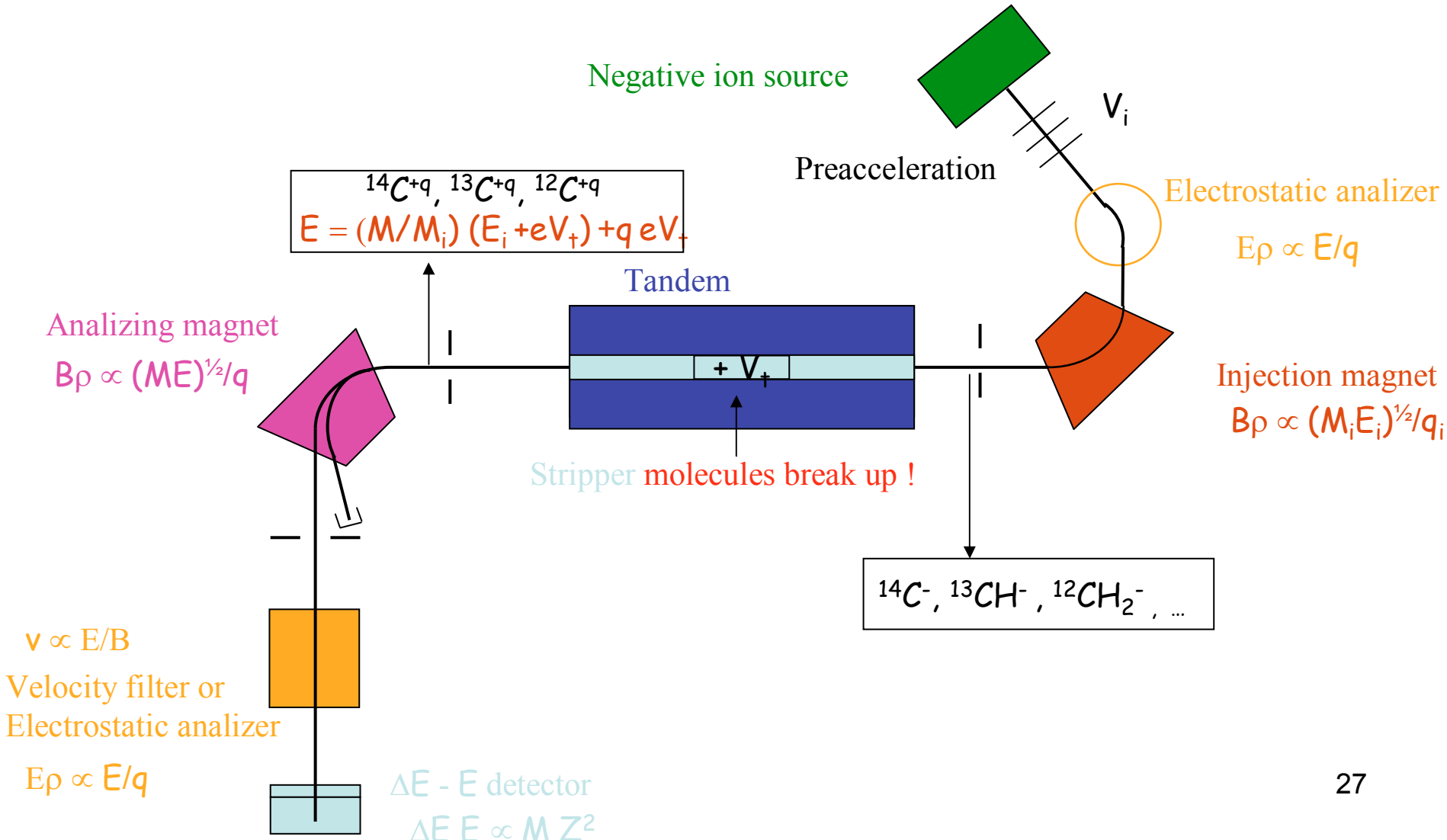

Atom counting

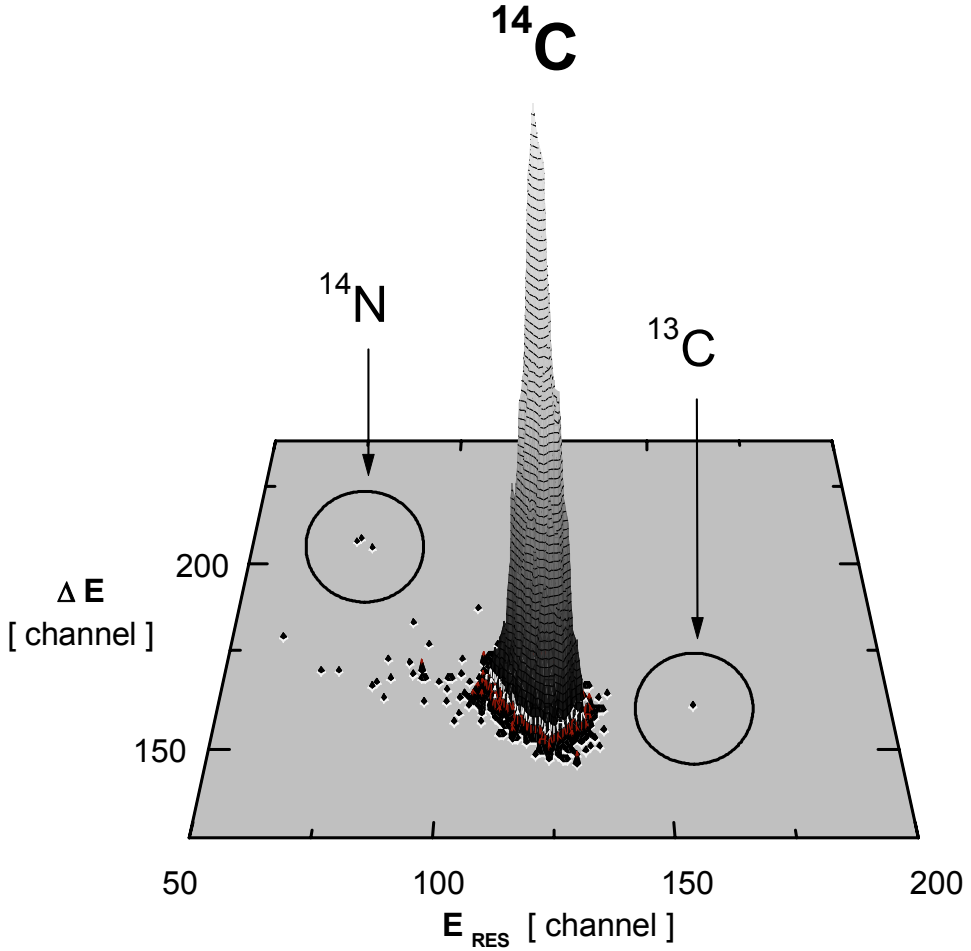

AMS detection of long-lived cosmogenic RN

Table 1.1 Long-Lived Radioisotopes Routinely Measured by AMS

Radioisotope	^{10}Be	^{14}C	^{26}Al	^{36}Cl	^{41}Ca	^{129}I
Half-life (a)	1.51 M	5.73 k	720 k	301 k	103 k	15.7 M
Stable isotopes	^{9}Be	^{12,13}C	^{27}Al	^{35,37}Cl	^{40,42,43,44}Ca	^{127}I
Stable isobars	^{10}B	^{14}N[a]	^{26}Mg[a]	^{36}Ar,[a] ^{36}S	^{41}K	^{129}Xe[a]
Chemical form	BeO	C	Al_2O_3	AgCl	CaH_2 /CaF_2	AgI
Sample size (mg)	0.5	0.02–1	2	1	10	2
Sensitivity (atom ratio)	2×10^{-15}	1×10^{-15}	2×10^{-15}	1×10^{-15}	5×10^{-15}	5×10^{-14}

[a] Do not form negative ions.

Accelerator mass Spectrometry
C. Tuniz et al., CRC Press, 1998

Sun

Historical, instrumental and proxy record

HISTORICAL RECORD

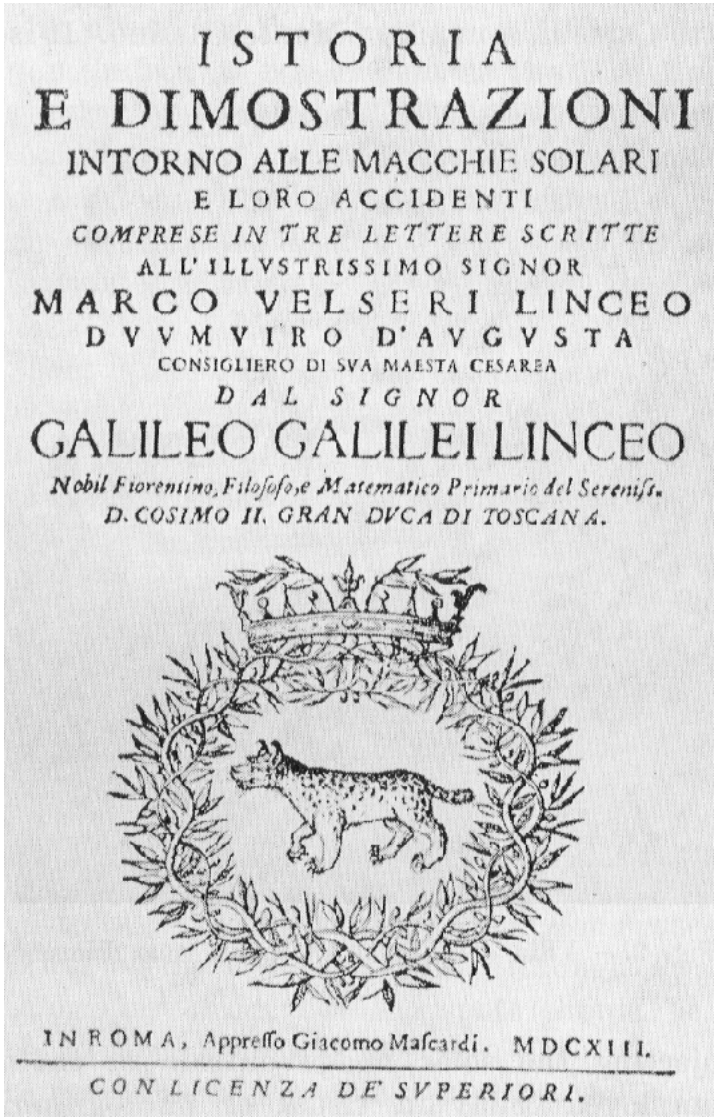

ISTORIA
E DIMOSTRAZIONI
INTORNO ALLE MACCHIE SOLARI
E LORO ACCIDENTI
COMPRESE IN TRE LETTERE SCRITTE
ALL'ILLVSTRISSIMO SIGNOR
MARCO VELSERI LINCEO
DVVMVIRO D'AVGVSTA
CONSIGLIERO DI SVA MAESTA CESAREA
DAL SIGNOR
GALILEO GALILEI LINCEO
Nobil Fiorentino, Filoſofo, e Matematico Primario del Sereniſs.
D. COSIMO II. GRAN DVCA DI TOSCANA.

IN ROMA, Appreſſo Giacomo Maſcardi. MDCXIII.

CON LICENZA DE' SVPERIORI.

1613

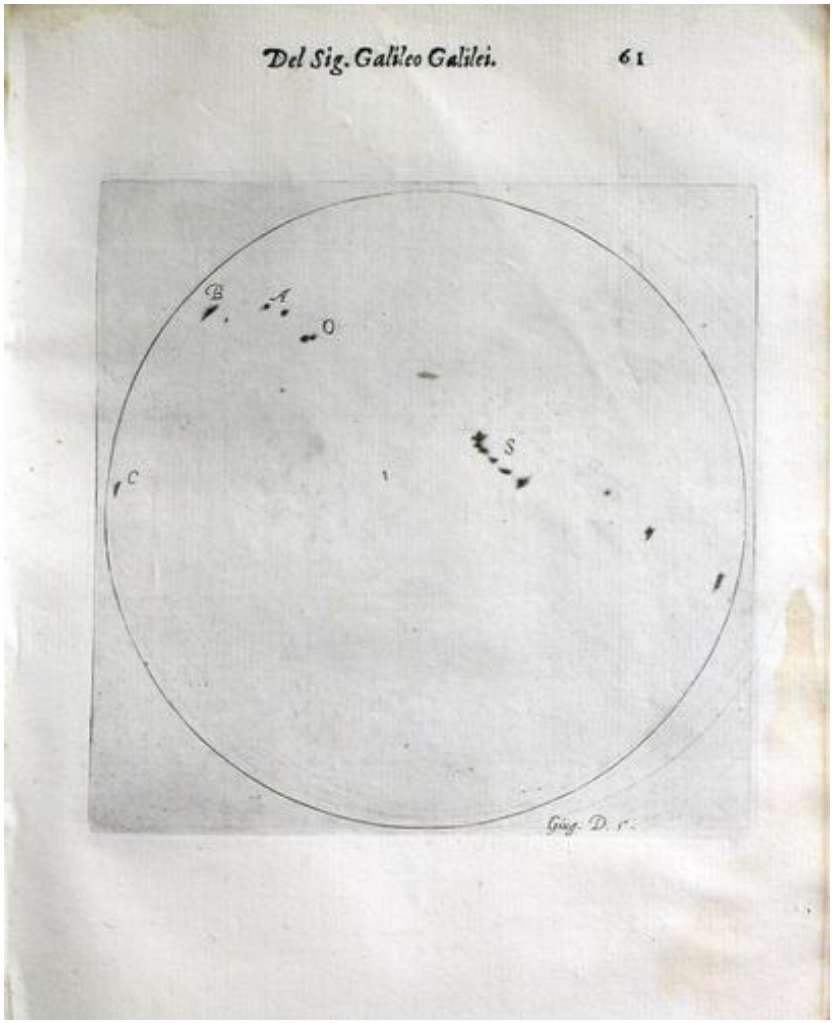

Annual mean sunspot numbers 1610-1987

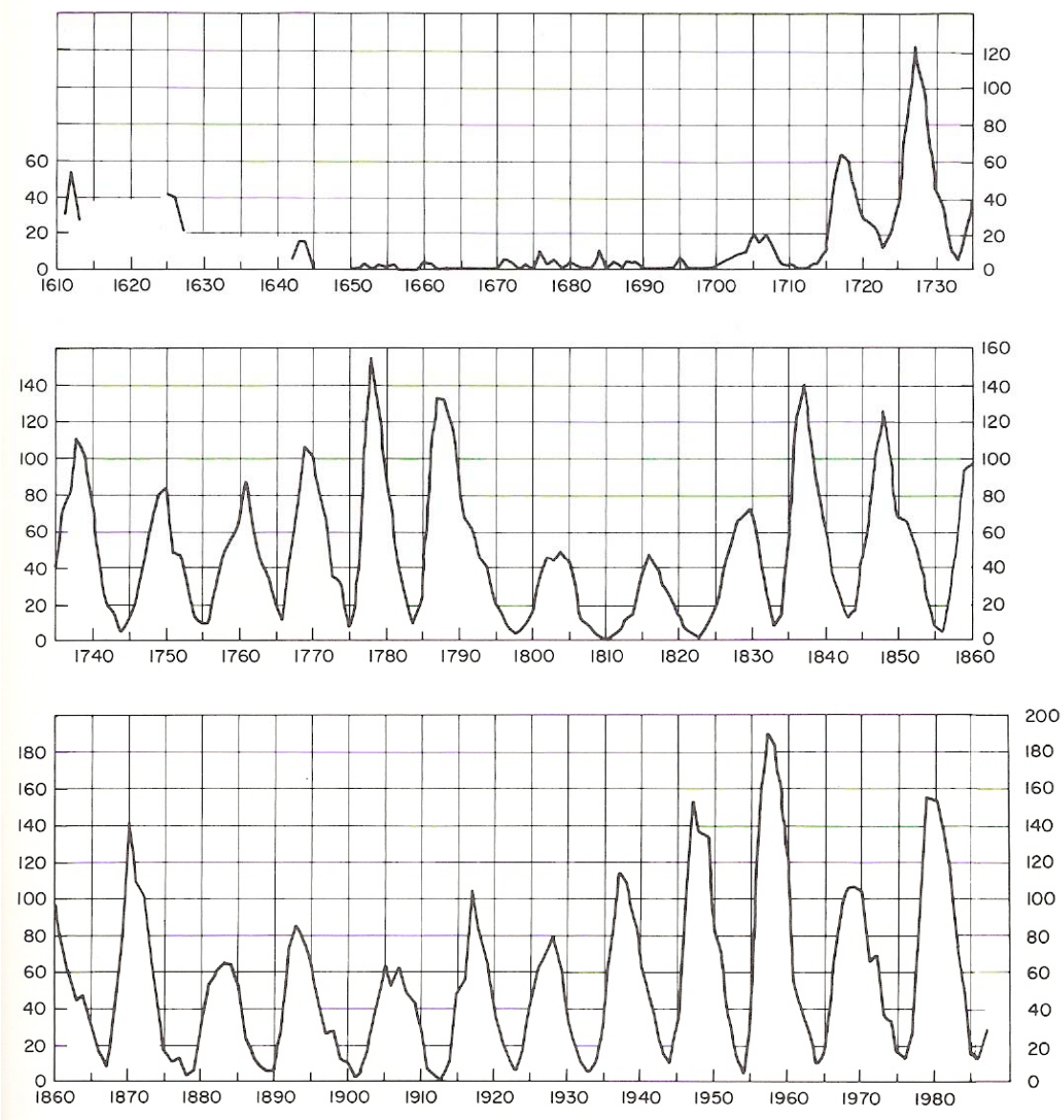

Cosmic Rays, M.W. Friedlander

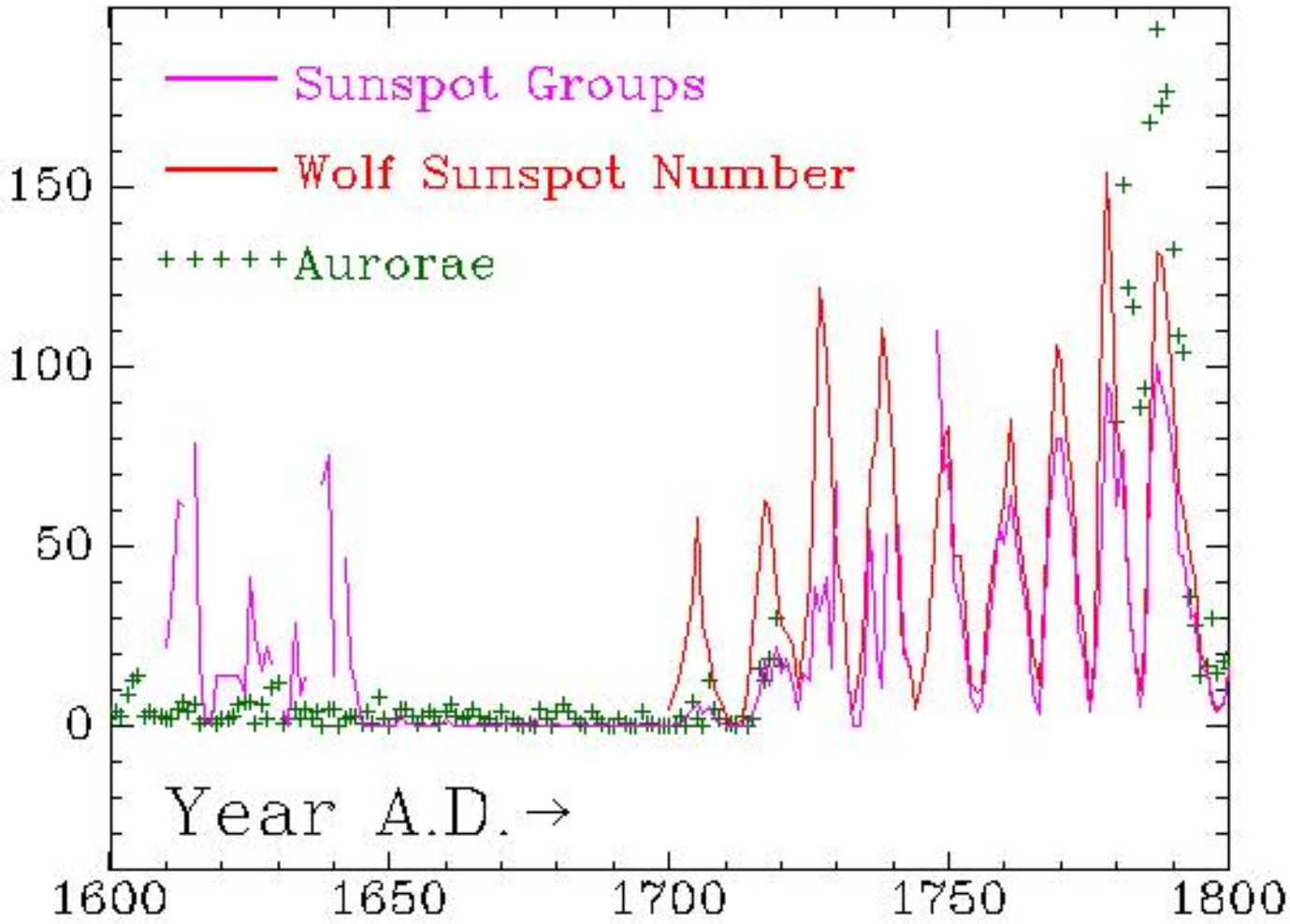
Sunspot Groups
Wolf Sunspot Number
+++++Aurorae
150
100
50
0
Year A.D.→
1600
1650
1700
1750
1800

INSTRUMENTAL RECORD

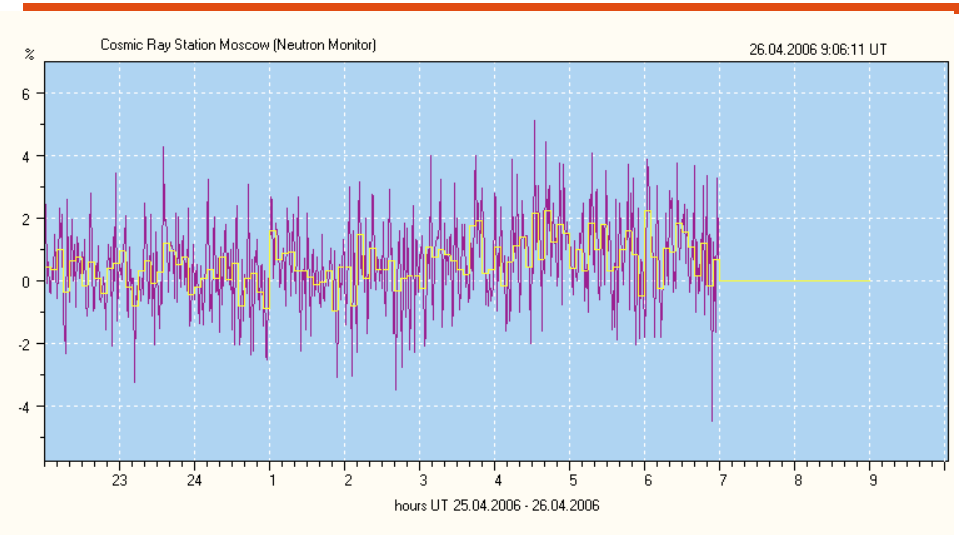

Moscow Neutron Monitor

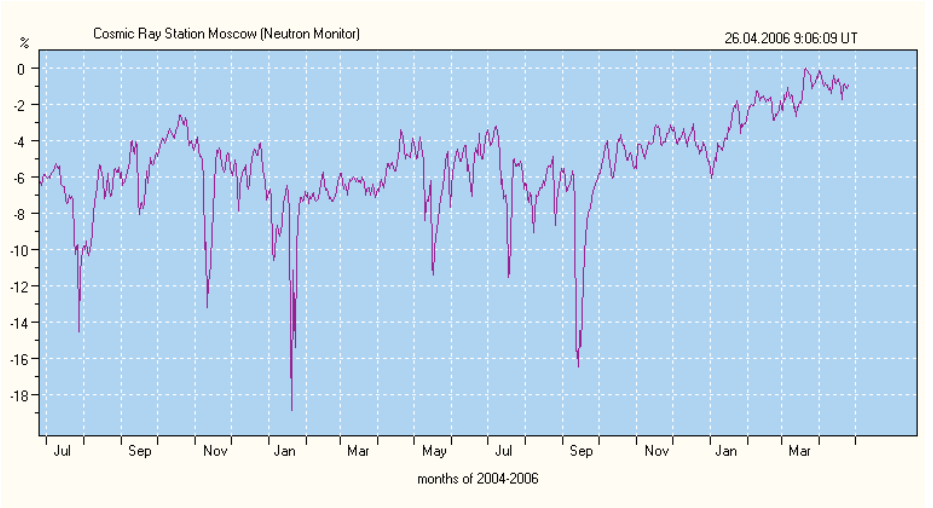

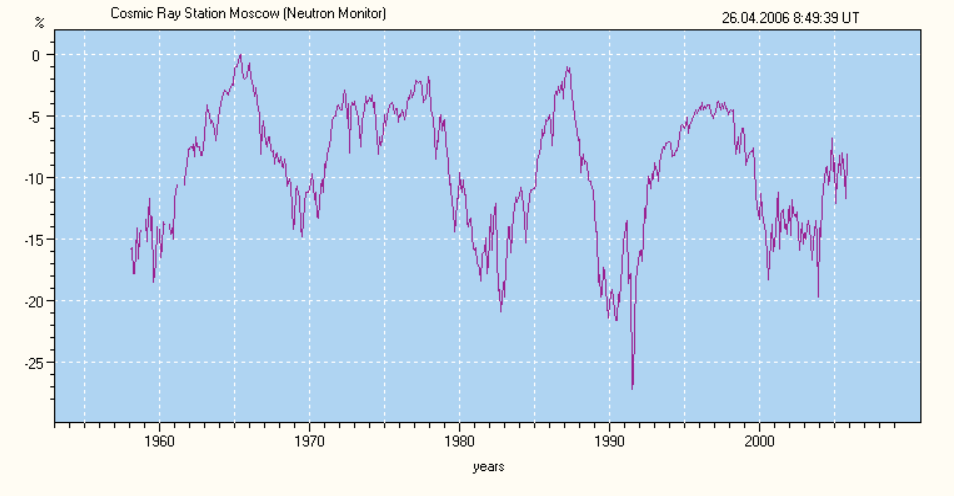

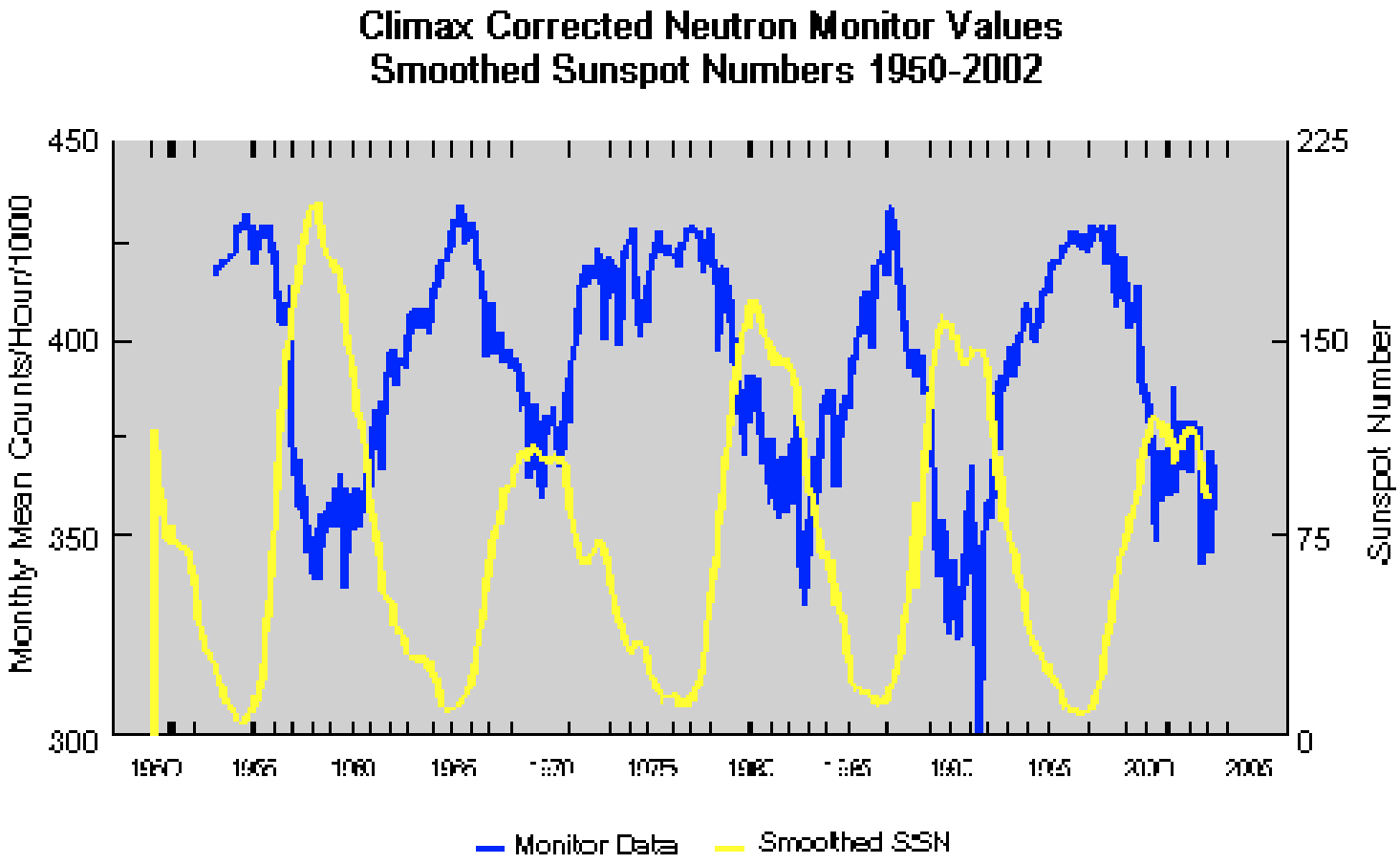
Climax Corrected Neutron Monitor Values
Smoothed Sunspot Numbers 1950-2002
Monthly Mean Counts/Hour*1000
Sunspot Number
450
400
350
300
225
150
75
0
1950
1955
1960
1965
1970
1975
1980
1985
1990
1995
2000
2005
Monitor Data
Smoothed SSN

PROXY RECORD

Tree Rings, Ice Cores, Sediments, Varves and Corals

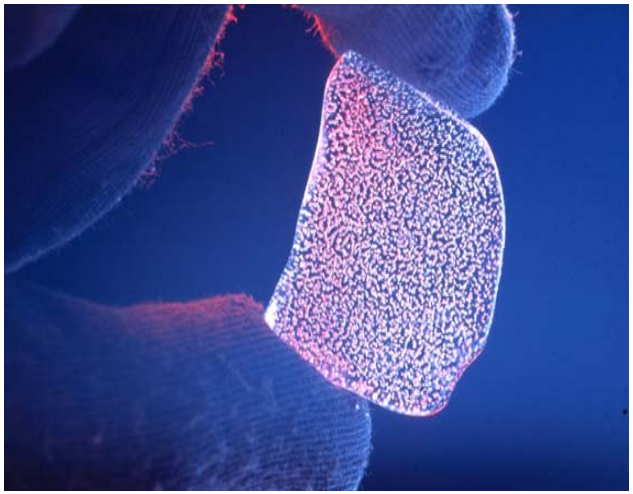

^{10}Be and ^{14}C production

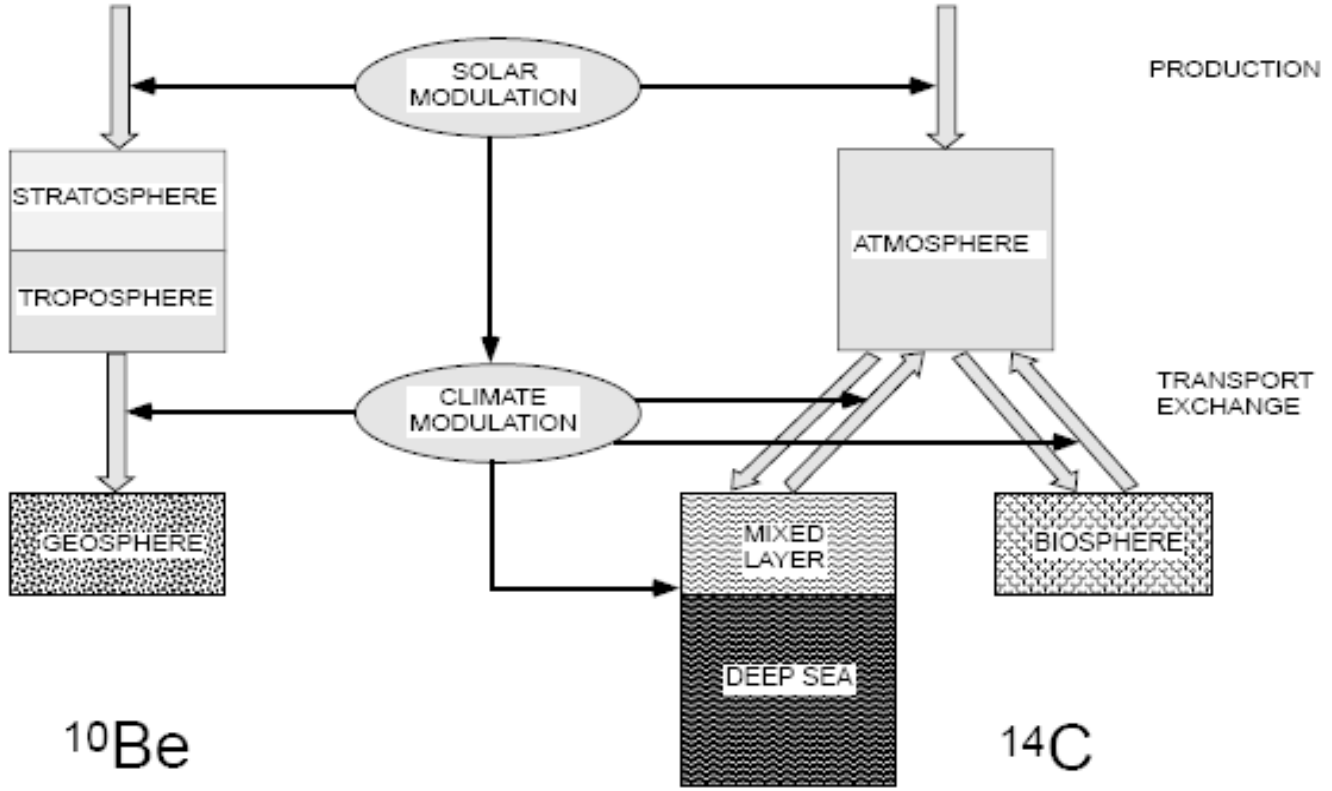

Figure 4. Description of the ^{10}Be and ^{14}C systems by simple box models. Solar modulation affects the production rate of both nuclides in a very similar way. Climate modulation (transport, atmospheric mixing, and deposition), however, leads to completely different effects in the two systems. After its removal from the atmosphere ^{10}Be becomes stored in the geosphere. In contrast ^{14}C continuously exchanges between the different reservoirs resulting in a much more complex behaviour.

Beer, Space Science Reviews, 2000

Long-lived cosmogenic radionuclides

Nuclide	Target	Half-life [y]	Production Rate [atoms $cm^{-2}s^{-1}$]	Inventory [tons]
^{14}C	N	5730	2	62
^{10}Be	N, O	1.51×10^6	0.018	105
^{36}Cl	Ar	3.08×10^5	0.0019	8

Beer, Space Science Reviews, 2000

^{10}Be production

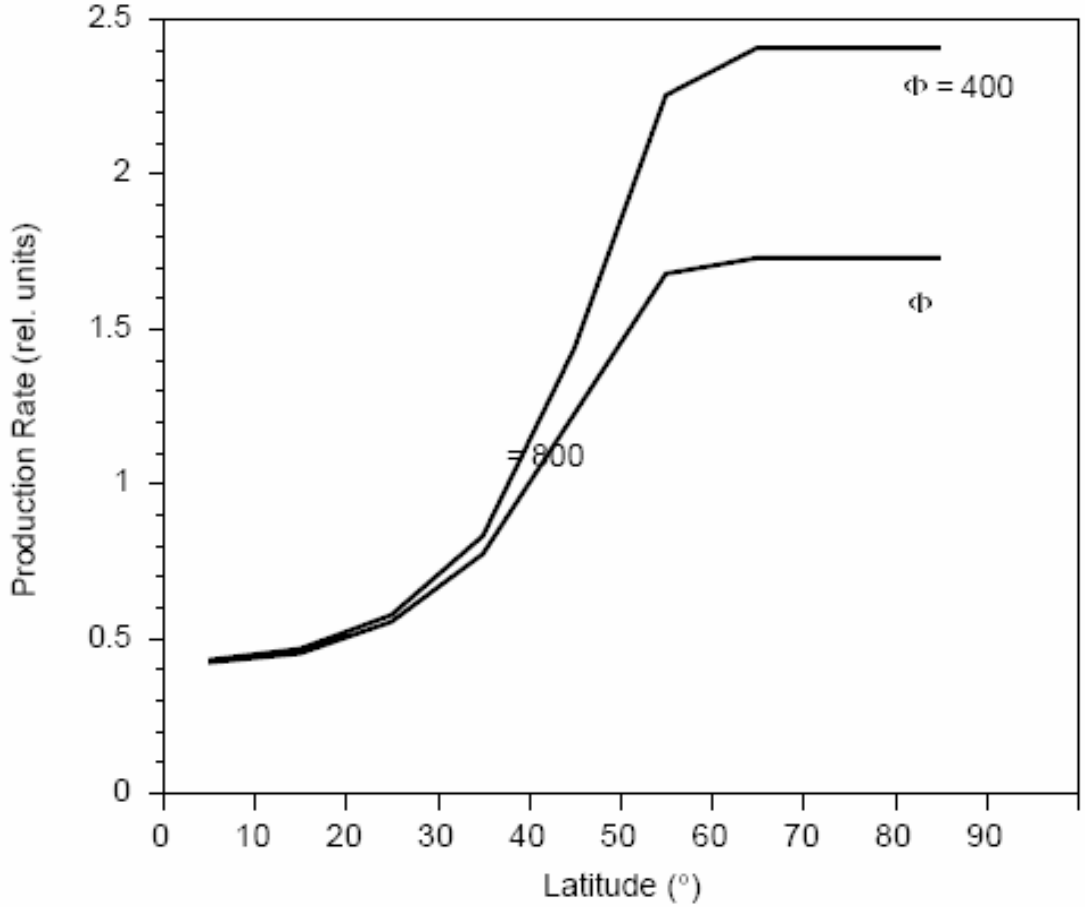

Figure 3. Relative production rate of ^{10}Be as a function of geomagnetic latitude for the present geomagnetic field intensity ($M = 1$) and two different solar activity levels. Note that the solar modulation is effective mainly at high latitudes.

Beer, Space Science Reviews, 2000

^{14}C in tree rings

Beer, Space Science Reviews, 2000

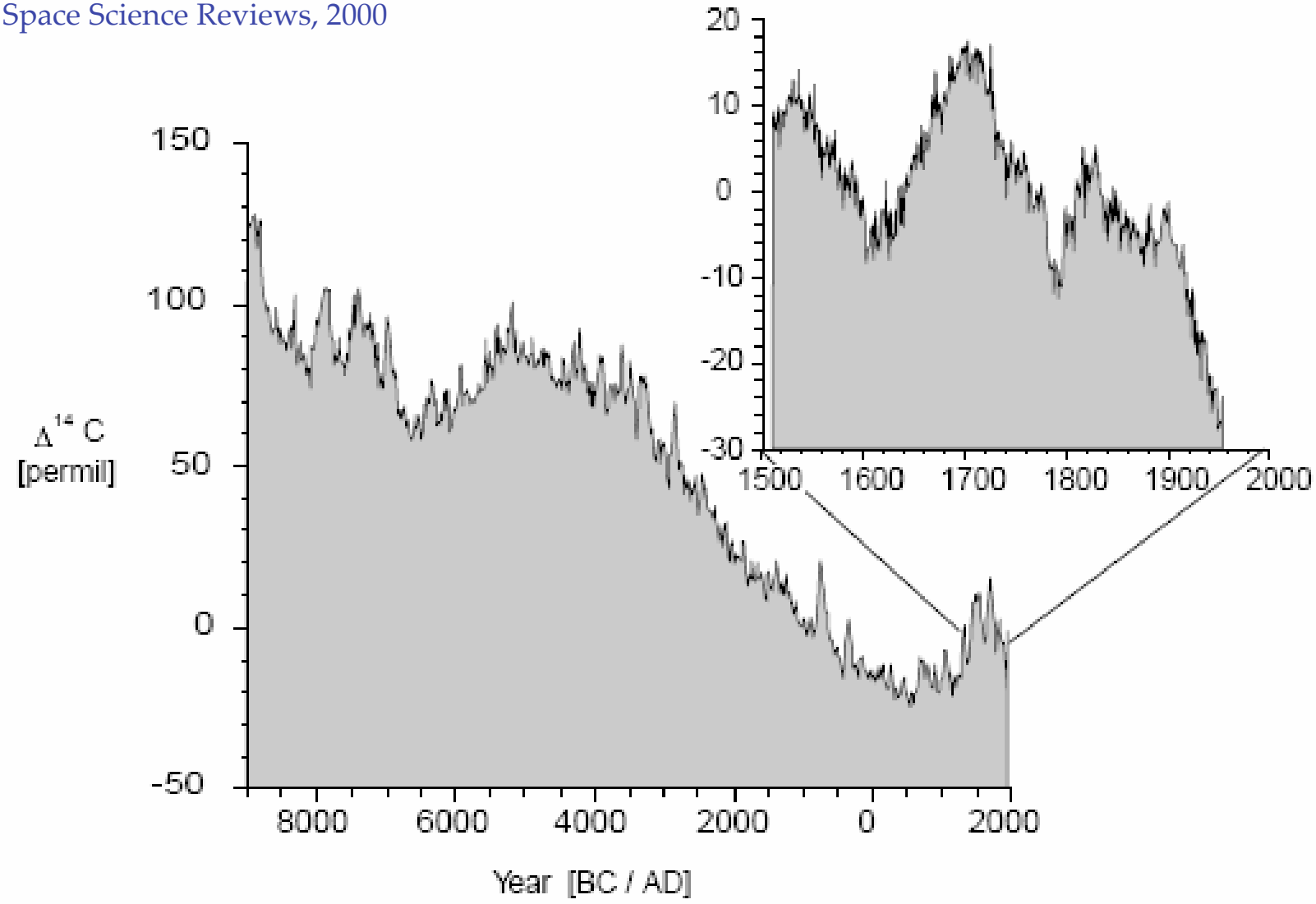

^{10}Be and ^{14}C record

Beer, Space Science Reviews, 2000

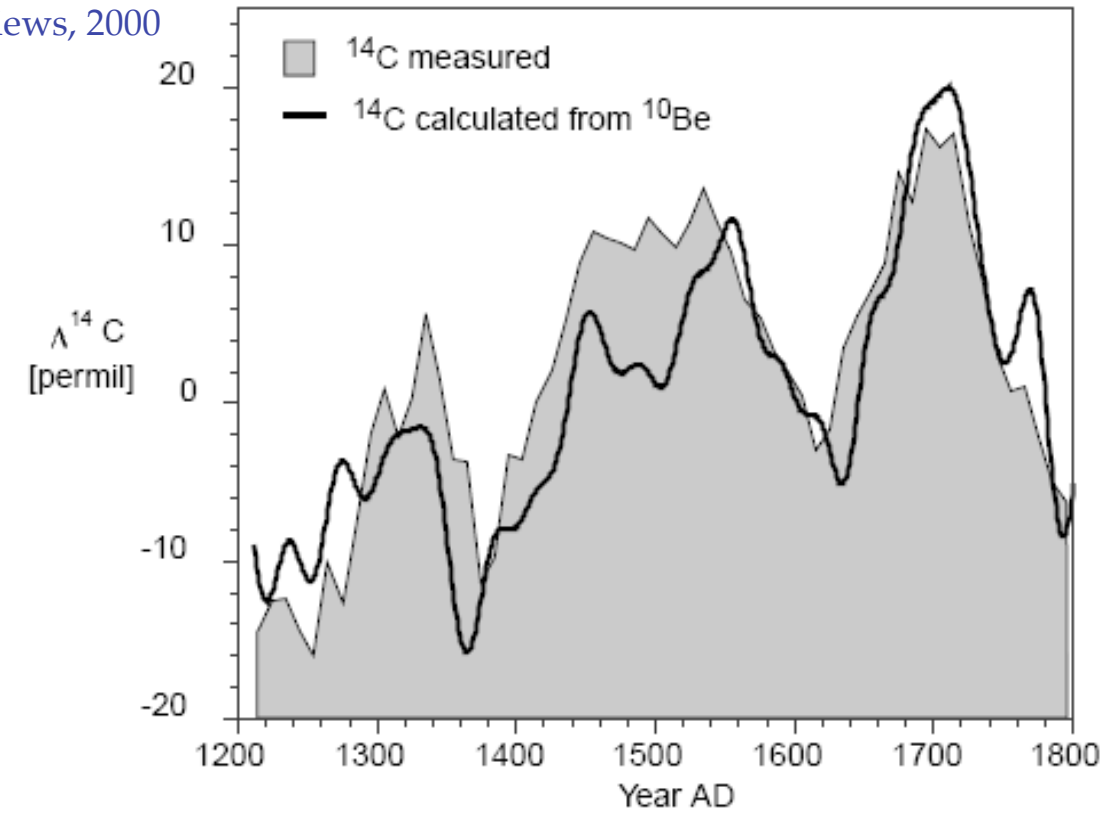

Figure 7. Comparison of the $\Delta^{14}C$ record measured on tree rings with the $\Delta^{14}C$ record calculated based on a combined ^{10}Be record of two ice cores from Milcent (Greenland) and the South Pole. The calculation was performed using the carbon cycle model of Fig. 4 assuming that the combined ^{10}Be record reflects directly the atmospheric production rate. The three periods of low solar activity (Maunder, Spoerer and Wolf) are clearly visible.

^{14}C in tree rings

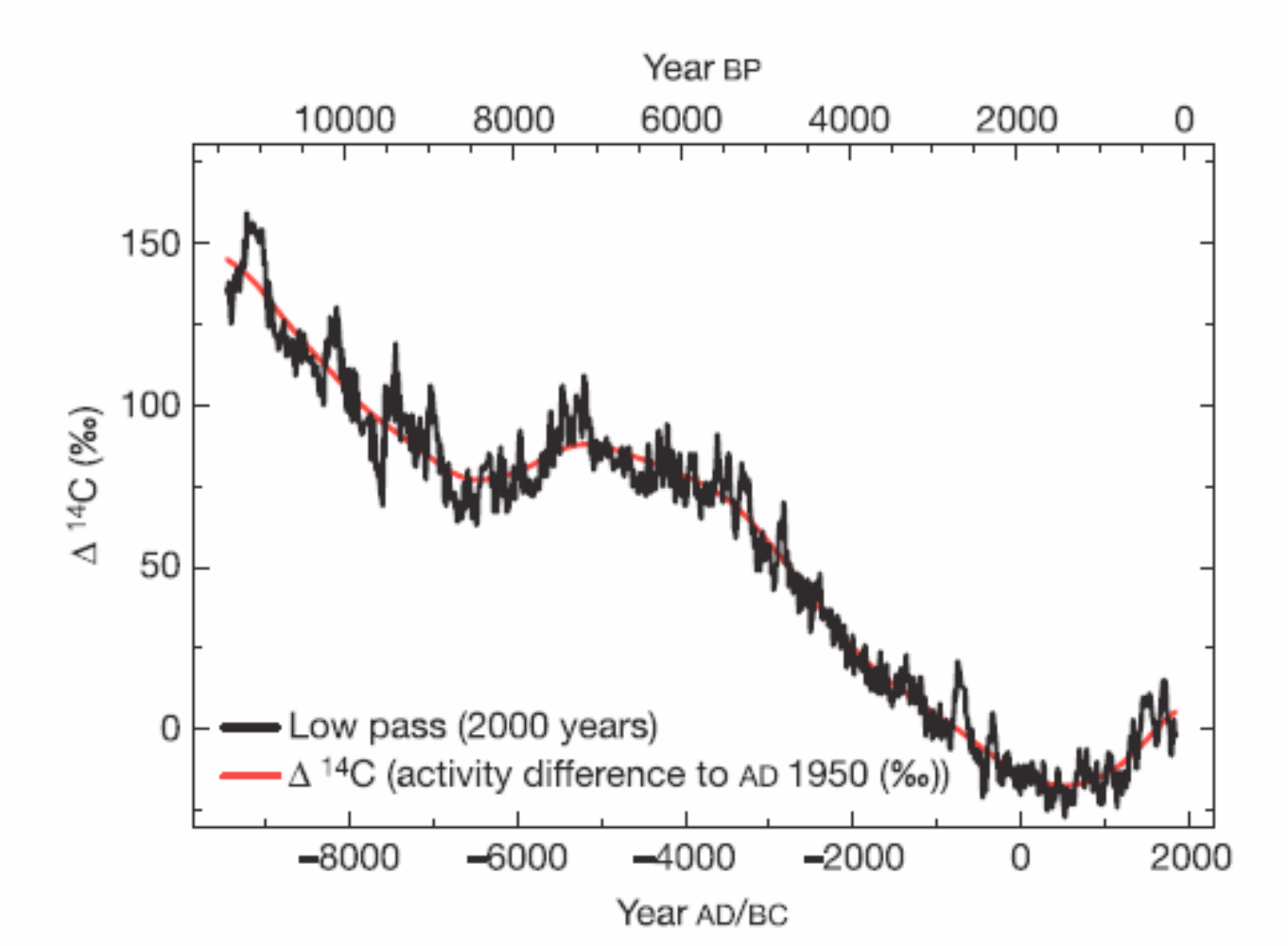

Solanski et al, Nature 2004

Unusual activity of the Sun during recent decades compared to the previous 11,000 years

S. K. Solanki[1], I. G. Usoskin[2], B. Kromer[3], M. Schüssler[1] & J. Beer[4]

Nature 2004

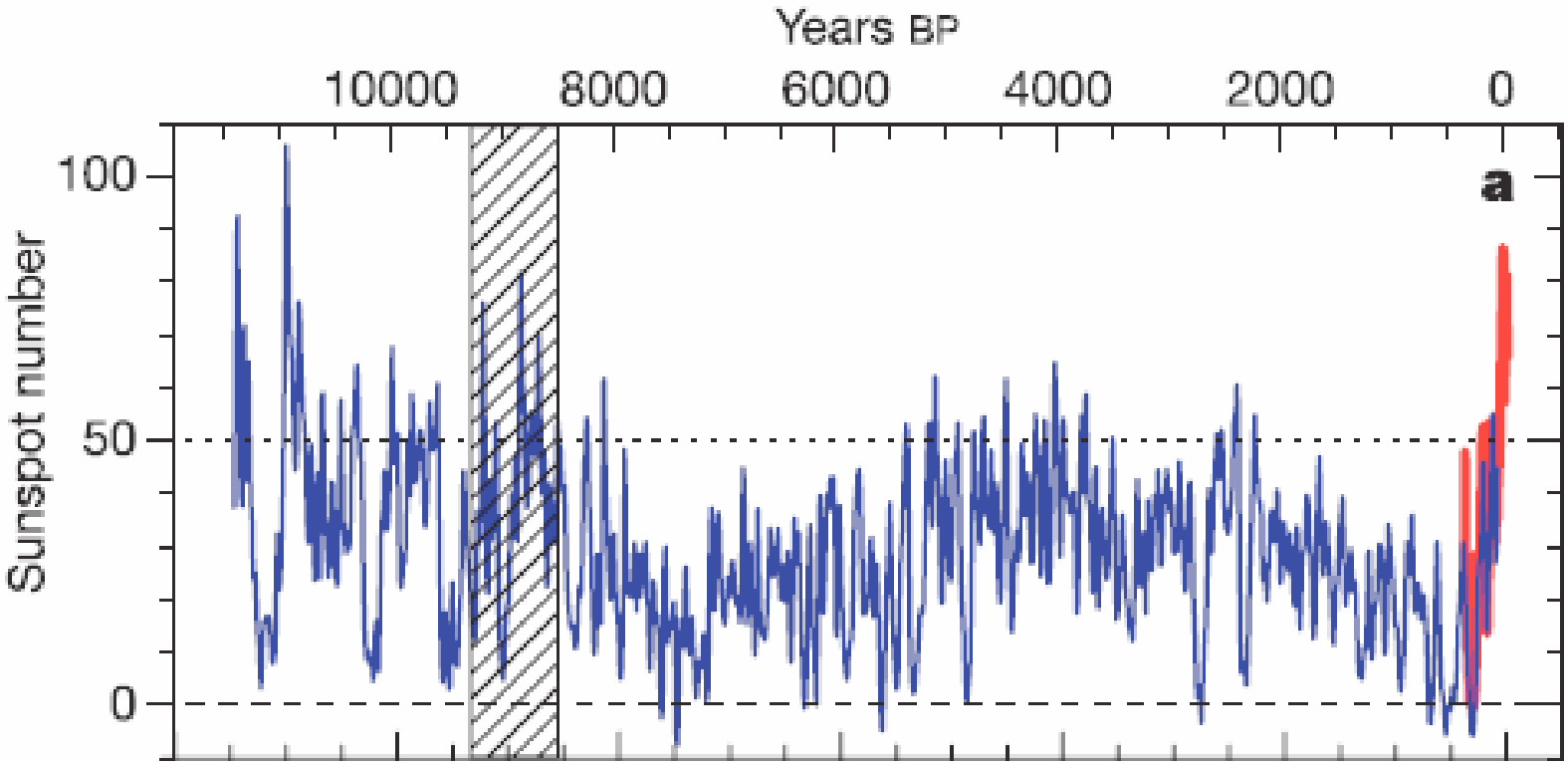

^{10}Be from the Sun

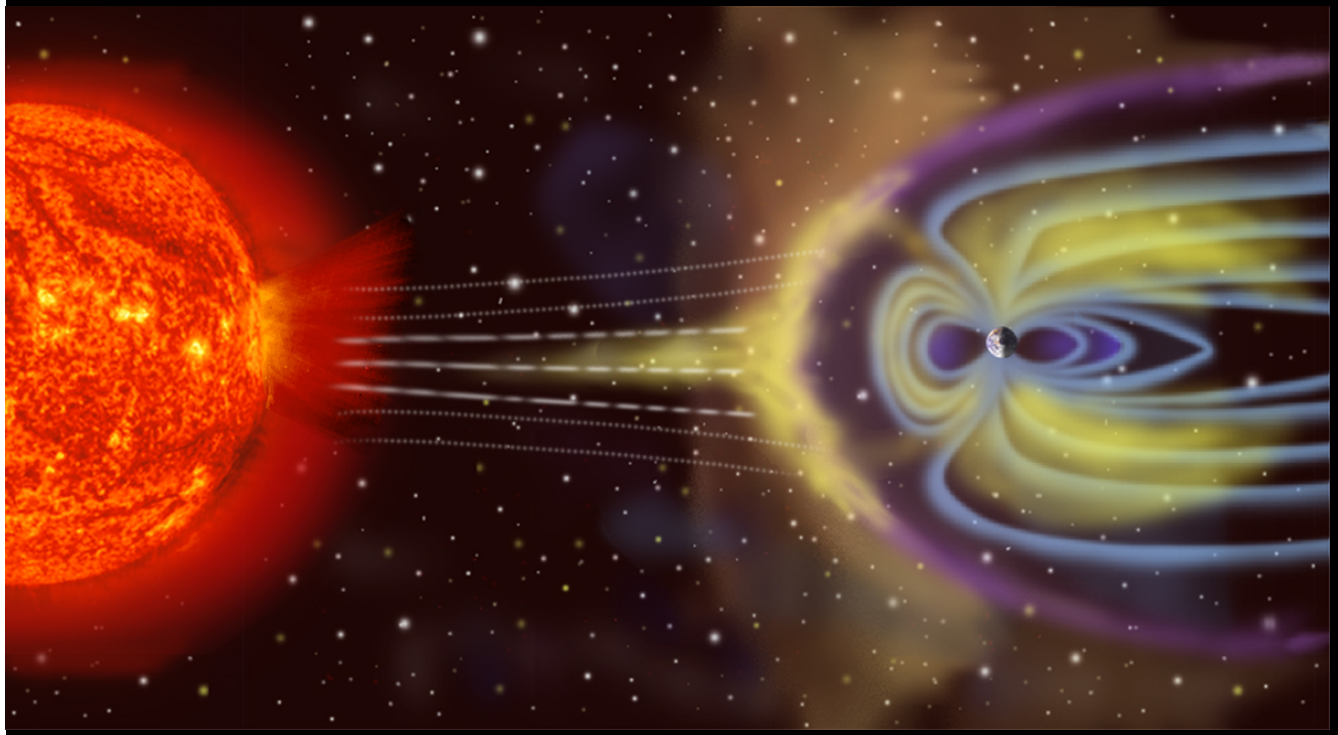

^{10}Be in excess of that expected from in situ cosmic ray spallation reactions is present in lunar surface soil 78481; This excess ^{10}Be and its association with surficial layers corresponds to 1.9 x 10(8) atoms per square centimeter, requiring a ^{10}Be implantation rate of 2.9 x 10(-6) atoms per square centimeter per second on the surface of the Moon. The most likely site for the production of this excess ^{10}Be is the Sun's atmosphere. The ^{10}Be is entrained into the solar wind and transported to the lunar surface

Thanks!